Available online at www.synsint.com

Synthesis and Sintering

ISSN 2564-0186 (Print), **ISSN** 2564-0194 (Online)

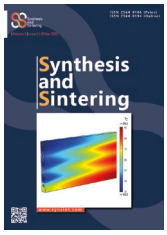

Review article

Synthesis and application of double metal MXenes: A review

Asieh Akhoondi [a,*], **Mitra Ebrahimi Nejad** [b, c,*], **Mohammad Yusuf** [d], **Tejraj M. Aminabhavi** [e], **Khalid Mujasam Batoo** [f], **Sami Rtimi** [g, h]

[a] *Department of Chemical Engineering, Arak Branch, Islamic Azad University, Arak, Iran*
[b] *Chemical Engineering Faculty, Tarbiat Modares University, P.O. Box 14115-111, Tehran, Iran*
[c] *Cracking and Catalysis Research Center, Tarbiat Modares University, P.O. Box 14115-111, Tehran, Iran*
[d] *Clean Energy Technologies Research Institute (CETRI), Faculty of Engineering and Applied Science, University of Regina, 3737 Wascana Parkway, Regina, SK S4S 0A2, Canada*
[e] *School of Advanced Sciences, KLE Technological University, Hubballi 580031, India*
[f] *King Abdullah Institute For Nanotechnology, King Saud University, Riyadh-11451, Saudi Arabia*
[g] *Ecole Polytechnique Fédérale de Lausanne (EPFL), 1015 Lausanne, Switzerland*
[h] *Global Institute for Water, Environment and Health (GIWEH), 1210 Geneva, Switzerland*

A B S T R A C T

MXenes are known as a new type of two-dimensional layered materials that are composed of carbide, nitride, or carbonitride of transition metals. In the recent discovery of a new class of MXenes, two transition metals occupy the metal site, called double transition metal MXenes (DTM). These multilayer composites are of interest due to their attractive features such as high ion transport, extensive surface area, and biocompatibility. Some computational methods are used to predict the properties and performance of bimetallic carbonitrides. The most important feature of this category of materials is the stability and amount of formation energy, which directly affects the choice of material in various applications. Density functional theory (DFT) calculations are very beneficial to estimate the thermodynamic stability of DTM MXenes. Of course, proper surface modification with stable terminals is needed to overcome the limitations of DTM MXenes. In this review, the electrochemical, metallic, and magnetic properties of DTM MXene have been presented first. In the following, preparation methods are summarized according to the latest published findings. Then, various applications including hydrogen evolution reactions, anode materials in lithium and sodium batteries, nanomagnetic materials, and special applications have been investigated. Finally, more challenges, prospects, and suggestions for the development of two-dimensional DTM MXenes have been presented.

KEYWORDS

MXene
Double-transition metal
Synthesis
Two-dimensional nanomaterials

OPEN ACCESS

1. Introduction

The two-dimensional structures or single-layer materials have significant differences in specific surface area, basic properties, and optical output (wavelength, intensity) compared to their counterpart solids [1]. 2D crystals such as graphene have received great attention in material science and engineering at the nanoscale, especially in semiconductors [2]. In two-dimensional materials, by reducing the thickness of the material even to one atom, major changes can occur in their properties [3]. Therefore, extensive studies have been conducted on the atomic structures, mechanical properties, behaviors, and defects of two-dimensional materials, which are the basis for their practical

* Corresponding author. *E-mail address:* asieh.akhoondi@gmail.com (A. Akhoondi), mitra.ebrahimi@modares.ac.ir (M. Ebrahimi Nejad)
Received 27 March 2023; Received in revised form 17 May 2023; Accepted 19 May 2023.

https://doi.org/10.53063/synsint.2023.32150

applications. It is predicted that thousands of crystals can be established from various solids by exfoliation, which is classified as two-dimensional materials [4].

In 2011, two-dimensional inorganic compounds called MXenes with the general formula $M_{n+1}X_nT_x$ were found from the family of transition metal carbides and nitrides atomically thin layers [5]. In the $M_{n+1}X_nT_x$ (n=1–3) systems, M is a transition metal and X is either C and/or N, terminated with T: –O, –F, –OH, and –Cl or bare. MXenes are synthesized through selectively acidic etching of the MAX phases ($M_{n+1}AX_n$, n=1–4), where A is an element of groups IIIA or IVA of the periodic table. A is mostly Al or Si in the layered hexagonal structure of MAX phases which is eliminated by HF acid [6]. At present, a large number of MXenes have been reported such as Ti_2CT_x, $Ti_3C_2T_x$, Nb_2CT_x, $Nb_4C_3T_x$, V_2CT_x, $Ta_4C_3T_x$, etc. [7]. While mainly titanium, niobium, and vanadium form the structure of MXenes, other metal elements such as Sc, Zr, Hf, and Mo are also predicted to form MXenes [8, 9].

Since MXenes have a high surface area per unit weight and electrical conductivity and hydrophilicity are their fundamental properties, they have found potential applications, especially in energy storage [10]. The ability to adjust the surface terminals of this type of two-dimensional materials has created a promising future in the preparation of thermoelectric devices [11], composites [12], photocatalysts [13], sensors, electrodes, batteries [14], nano-magnets, supercapacitors [15], and membranes. The semiconductor nature and unique physicochemical properties of these compounds have led to their use in photocatalysis in order to accelerate redox reactions such as hydrogen evolution reactions and other photocatalyst-based usages [16]. Moreover, as two-dimensional emerging materials, MXenes have potential applications in biomaterials nanomedicine [17], and photothermal conversion [18].

In the group of MXenes, other solutions have been invented; where two transition metals occupy the M positions which differ from their single transition metal counterparts [19]. The two intermediate metals are distinguished by M′ and M" and these semiconductors are divided into in-plane and out-of-plane groups (ordered DTM MXenes), and solid-solution DTM MXenes based on their structure. The behavior of these three groups of DTM MXenes is different from single metal MXenes, which can have various uses in the future. The purpose of this review is to investigate the characteristics, design, and synthesis methods of double-transition metal MXenes (DTM) and their hybrids in composite configuration with growing applications from electrocatalyst to energy storage.

2. Basic properties

MXenes have a high stability because they are synthesized under strongly acidic (HF) conditions [20]. It should be noted that the stability in bimetallic MXenes depends on the type and content of each of the constituent metals. For instance, in Fig. 1, the stability of $Mo_xV_{4-x}C_3$ is shown for different values of x [21]. According to this figure, V_4C_3 is stable throughout the molybdenum-containing region. Moreover, MXenes offer a unique combination of metallic conductivity and hydrophilicity that have already shown promise as electrodes for supercapacitors and Li-S batteries. The developed composites based on carbonitride MXenes have high resistance under high-temperature oxidation [22]. In this regard, TiCrC with a Ni-Cr additive has been investigated. It has been recommended that cladding technology with a Ni-P alloy be used to decrease the intensity of the composite oxidation. In addition, MXenes have a large surface area and high electron mobility, which promises a wide range of applications in the future.

The results of DFT calculations and experimental methods have shown that doubly ordered carbonitrides are thermodynamically more stable than solid solution counterparts [8]. The characteristics and properties of DTM MXenes are distinguished among existing 2D materials by carefully engineering the composition, the number of metal sheets, interlayer space, and terminated group functionalities [23]. Furthermore, the electronic thermal conductivities of DTM carbonitrides revealed by Boltzmann's transport theory differ with single metal MXenes. In one case, the Ti layers have been covered with

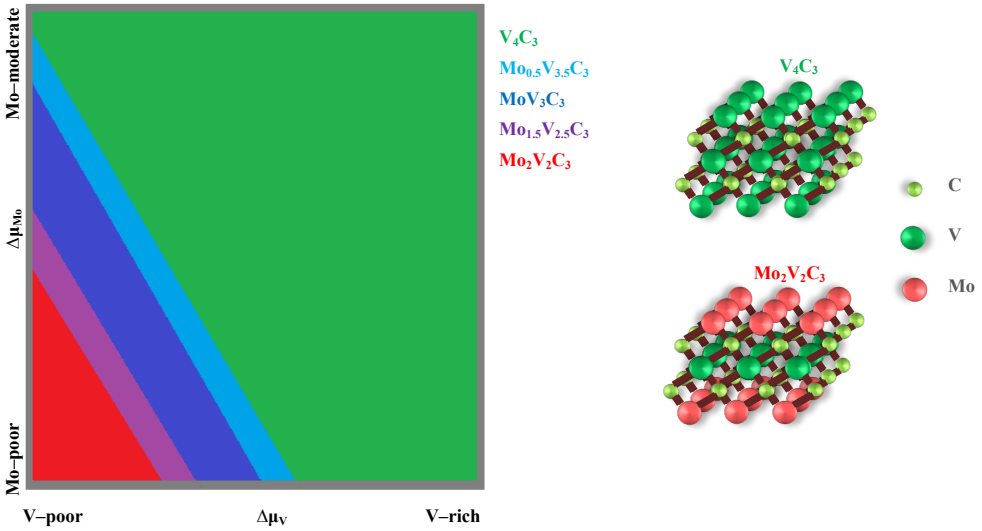

Fig. 1. Phase diagram for the thermodynamic stability of the different $Mo_xV_{4-x}C_3$ MXenes.

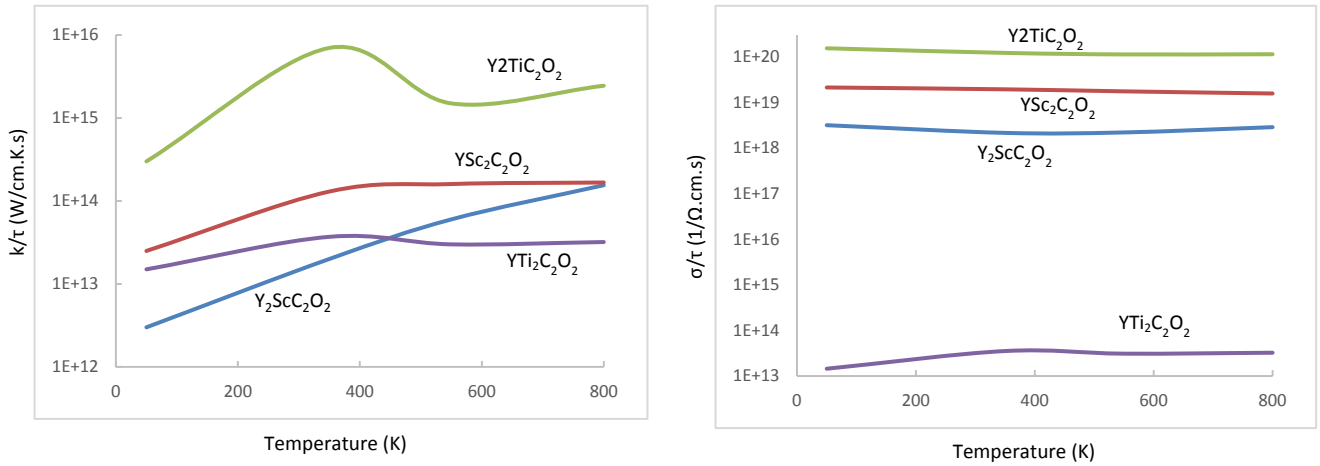

Fig. 2. Electrical and thermal conductivities variations of $Y_2ScC_2O_2$, $Sc_2YC_2O_2$, $Y_2TiC_2O_2$, and $Ti_2YC_2O_2$.

Y atoms in $Ti_3C_2O_2$ to modify the electronic structure and transport characteristics [24]. In addition, $TiY_2C_2O_2$ MXene has higher electrical conductivity compared to $Ti_2YC_2O_2$ because of its squared band velocity. This phenomenon also applies to $Sc_2YC_2O_2$ and $ScY_2C_2O_2$, whose functional group is –O (Fig. 2). On the other hand, Chang et al. [25] calculated the semiconductor properties of $ScYCT_2$ (T: F and OH) and bandgap and believe that $ScYCF_2$ and $ScYCOH_2$ are stable and has better thermoelectric properties. In another study, Caffrey [26] has shown the effect of different types of terminating groups on the stability of DTM MXenes. In his research, it was found that $Mo_2Ti_2CT_x$ is stable in a wide range of pH in aqueous solution. In contrast, $Cr_2Ti_2CT_x$ and $Cr_2V_2CT_x$ are only stable at pH<7 when T is restricted to the –F functional group. But in the case of $Mo_2Sc_2CT_x$, if scandium ions interact with F ions in the solution and form ScF_3, this MXene cannot be stable under acidic pH. In addition, Mo_2ScC_2 and its functionalized congeners meet the criteria of mechanical stability. If oxygen is the surface terminal, it can be a suitable option for ultra-sensitive sensors [27].

According to a comprehensive evaluation of surface modification, Dihingia et al. [28] have found that –O functionalized carbonitrides are the most durable systems (Fig. 3). The second stable group is the fluorine surface functional class, and MXenes with –OH terminal are the least stable types except for the W-based/$MoCr_2$ carbide and nitride compounds. It has been experimentally proven that 2D materials have almost all the properties observed in bulk materials except magnetic behavior [29]. As two-dimensional composites, MXenes have great potential to achieve intrinsic magnetism due to their chemical and structural diversity [30].

3. Synthesis and design

Since DTM carbonitrides can be pristine or with multiple surface end groups, they have many varieties. The type of pair of transition metals greatly affects the energy of formation [31]. Geng et al. acknowledged that MXene monolayers with oxygen functional groups are easily constructed due to low formation energy (E_f), while $M_2M'C_2$ with boron end groups have the highest formation energy [32]. Most $M_2M'C_2$ functionalized with N, S, and P have positive or negative

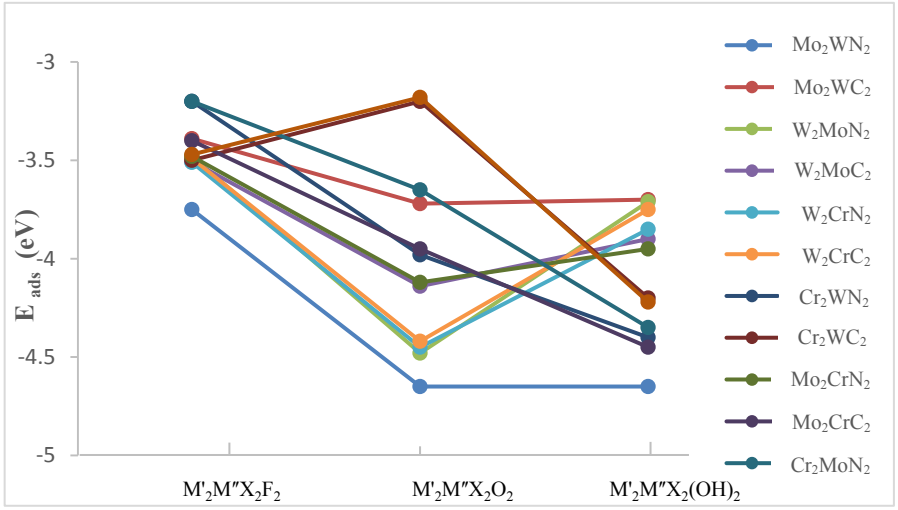

Fig. 3. The adsorption energies of terminated systems with –OH, –F, and –O groups onto the surfaces of Cr-Mo, Cr-W, and W-Mo MXenes.

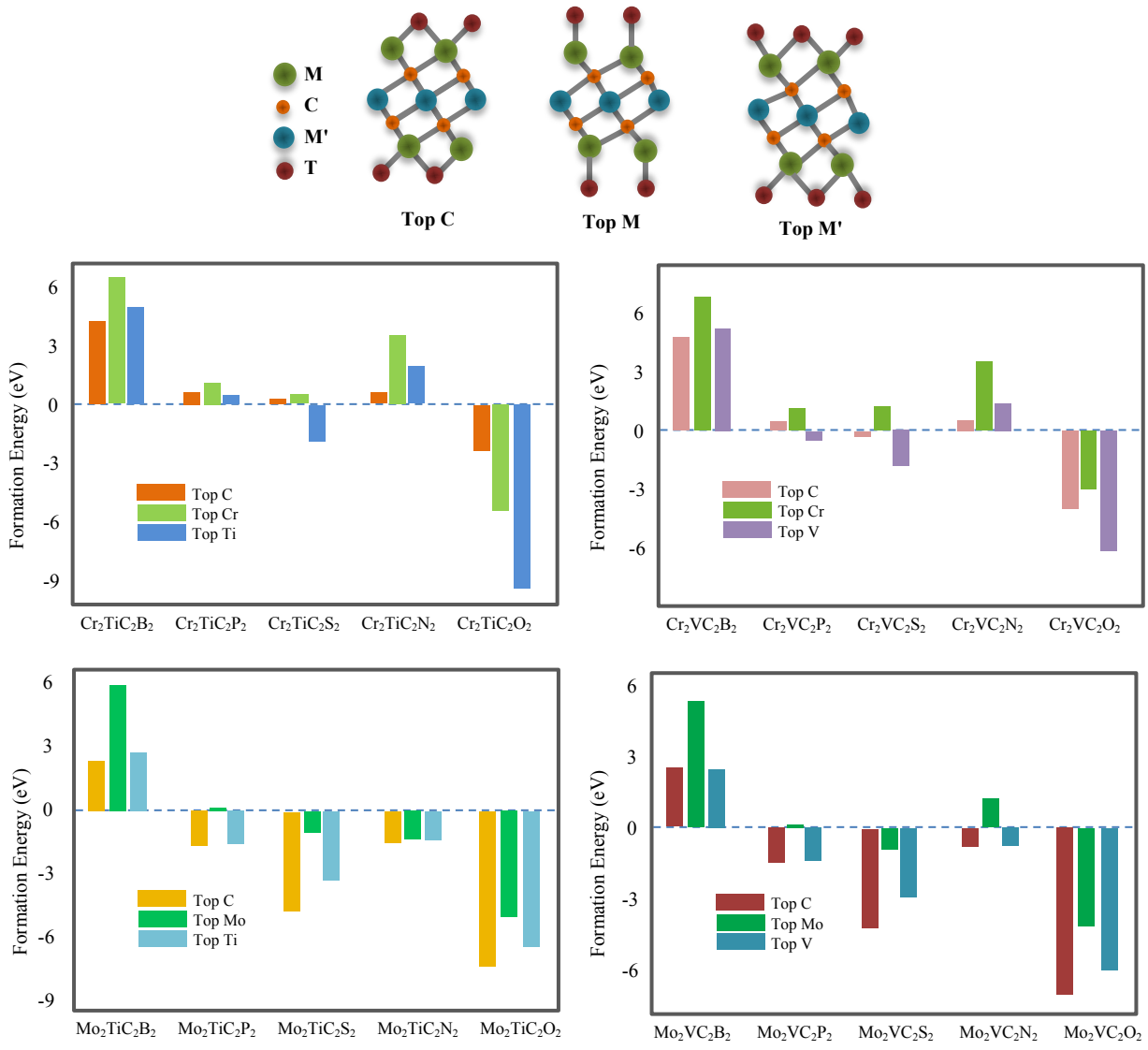

Fig. 4. Top and side view of 2D $M_2M'C_2$ and the formation energies of $Mo_2TiC_2T_x$, $Mo_2VC_2T_x$, $Cr_2TiC_2T_x$, and $Cr_2VC_2T_x$ monolayers.

formation energy except $Mo_2VC_2N_2$, $Cr_2VC_2S_2$, and $Cr_2MC_2N_2$ with top Ti and V configuration (Fig. 4). Alternatively, E-etching (electrochemical etching) offers a favorable, practical, fast, and environmentally gentle technique for aluminum removal [33]. In the following, various synthesis routes of DTM MXenes are summarized.

In one case, the different elemental molar ratios of Nb:Mo have been mixed with a constant molar ratio of Al:C and sintered at high temperatures for several hours under argon flow to achieve MAX phases [34]. After the successful exfoliation of aluminum layers in MAX phases to produce $Mo_{2+\theta}Nb_{2-\theta}C_3T_x$, two strategies can be used to convert MXene layers into flake-shaped monolayers: 1) utilization of HF/HCl with delamination agent (LiCl) and 2) solution of HF/tetramethylammonium hydroxide (TMAOH). Flake sizes of different $Mo_{2+\theta}Nb_{2-\theta}C_3T_x$ synthesized HF/TMAOH are shown in Fig. 5 with the comparison of the current density of Mo_2CT_x and $Mo_{1.33}CT_x$ produced from references [35] and [36]. The $Mo_{2.5}Nb_{1.5}C_3T_x$ has the highest electrical conductivity even more than bare $Mo_2Ti_2C_3T_x$, indicating some changes in the electronic structure.

MAX phases contain strong layer bonds that require a strong etch. The synthesis of carbonitrides can be achieved through a wet chemical method for etching selective layers from their precursor MAX phase at RT or above. In the research conducted on the charge transfer resistance of $Mo_2TiC_2T_x$ and $Mo_2Ti_2C_3T_x$, the wet chemical method has been used for synthesis in a Teflon bottle containing HF immersed in an oil bath [37]. The etched powder has been stirred, washed, and centrifuged to obtain exfoliated MXene. Electron impedance spectroscopy (EIS) of $Mo_2Ti_2C_3T_x$ has shown higher charge transfer resistance than $Mo_2TiC_2T_x$ (Fig. 6). Hence it is predicted that $Mo_2TiC_2T_x$ has a rapid kinetic and better catalytic performance for HER and OER.

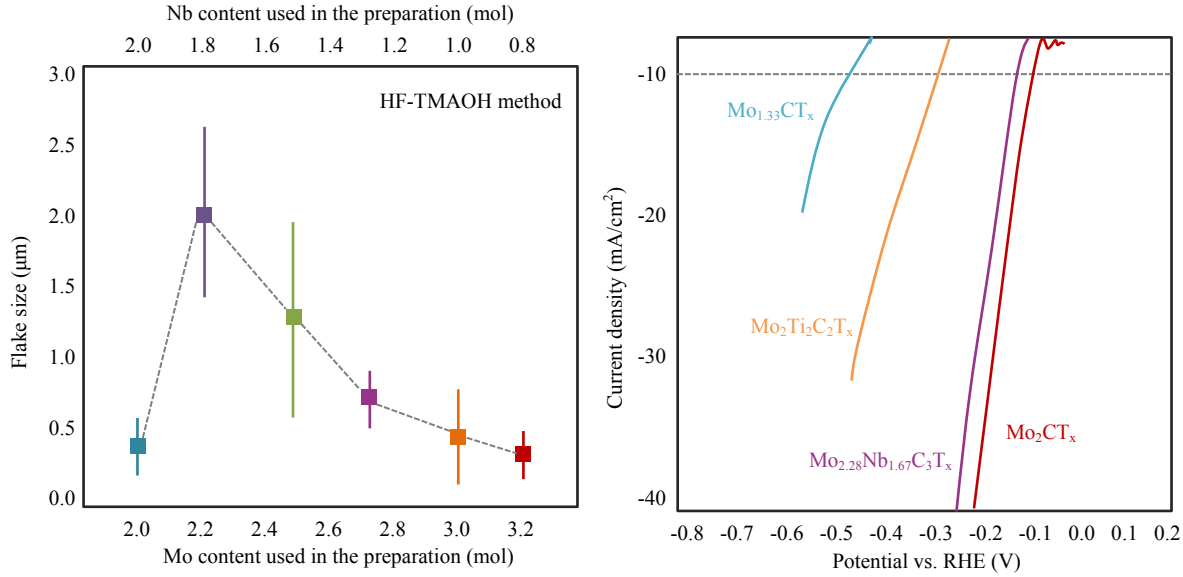

Fig. 5. a) Flake sizes of $Mo_{2-\theta}Nb_{2-\theta}C_3T_x$ prepared through HF-TMAOH etching and b) potential vs. current density plots of $Mo_2Ti_2C_3T_x$ and $Mo_{2.28}Nb_{1.67}C_3T_x$ compared to Mo_2CT_x and $Mo_{1.33}CT_x$.

The hydrothermal method is one of the most powerful and widely used for the production of nanostructures, which has received a lot of attention today due to its simplicity and cost-effectiveness [38]. As is known from the name of this method, the synthesis based on the formation and growth of crystals, takes place in water at a moderate or high temperature above RT [39]. Therefore, Ma et al. [40] adopted this method in order to deter the destruction of the original layered construction of MXene after etching with hydrofluoric acid to prepare TiNbC MXene. Hydrothermal pretreatment on $TiNbCT_x$ also prevents abnormal grain growth by direct calcination in the air. Next, the TiNbC suspension is freeze-dried to obtain black powder. The variables in the hydrothermal process are the type of water, temperature, time, surfactant, and pH, which have key roles in product quality [41]. The ratio of Nb to Ti in Ti-Nb carbides significantly influences the fabricated composition, but it does not have a direct relationship with the stoichiometry of MXene [42]. The TiNbC colloidal precipitate with Nb and TiO_2 is placed in an insulated container to synthesize Nb-doped TiO_2/TiNbCO as a new type of composite at high temperatures for several hours. In the following, the output solution from the autoclave is heated in an oven to get the final powder [43]. The degree of oxidation of TiNbC can be tuned by temperature controlling, and the oxide nanolayers turn dense with the increase in temperature. The strength junctions of TiNbCO and Nb-doped-TiO_2 nanosheets are ensured through the in-situ partial oxidation [44]. Moreover, the components' synergy and electrochemical activity are improved with double metal MXene and metal oxide [45]. However, it has been found that the electrical conductivity and hardness of the TiNbC composite that is combined with SiC significantly increases [46]. To investigate

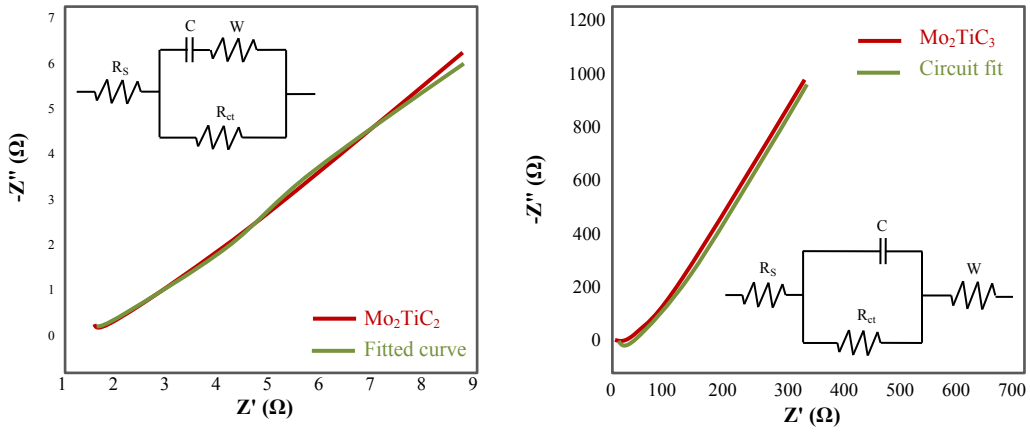

Fig. 6. Electron impedance spectroscopy together with fitted equivalent circuits of $Mo_2Ti_2C_3$ and Mo_2TiC_2.

the properties of TiNbC-SiC composite, Fides et al. used the hot pressed method for synthesis in two steps without adding sintering additives. The results of electrical discharge machining (EDM) of the samples indicate the readily machinable composite but severe oxidation of the cuttings, which indicates that more surface treatment is needed. In another research, Andrade and co-workers [47] synthesized solid solution $Nb_yV_{2-y}C$ by selective etching of niobium and vanadium with a controlled ratio, next by oxidation and dissolution in H_2O_2 and recrystallization by hydrothermal process. They demonstrated the construction of a solid solution boosted the etching kinetic of MAX phases and facilitated the carbide formation compared to pristine V and Nb MXenes.

In another study, Mo_2TiAlC_2 powder was used in an aqueous concentrated hydrofluoric acid to prepare $Mo_2TiC_2T_x$ MXene [48]. After mixing and washing with distilled water, the obtained solution was centrifuged to reach the desired acidity (pH=6–7). Next, the water in the suspension is completely removed by the freeze-dried method. For the exfoliation of $Mo_2TiC_2T_x$, $(C_4H_9)_4NOH$ as an organic solvent has been used. After stirring for one day, the solution was centrifuged and washed with water to eliminate the solvent. The synthesis method of $Mo_2TiC_2T_x$-molybdenum vacancy (V_{Mo}) is an electrochemical exfoliation technique in which the deposition of $Mo_2TiC_2T_x$ on an electrode serves as the working electrode. Meanwhile, by creating molybdenum vacancies, platinum atoms can be anchored in their place. In order to prepare $Mo_2TiC_2T_x$-single Pt atoms (Pt_{SA}), in-situ electrochemical exfoliation and atom trapping strategy have been employed in a three-electrode system. The XANES measurement of the electronic state of the Pt species in Fig. 7a exhibits higher intensities of $Mo_2TiC_2T_x$-Pt_{SA} compared to Pt foil and PtO2. Fig. 7b shows the Fourier transforms of the Pt edge, which indicates $Mo_2TiC_2T_x$-Pt_{SA} has no Pt particles or clusters.

4. Applications

4.1. Hydrogen evolution

Sustainable producible clean hydrogen is a promising alternative energy carrier to replace carbon-based fuels [49]. Hydrogen production by water splitting with an electrocatalytic approach can become more sustainable after discovering new materials, such as 2D nanomaterials [50]. Developing environmentally friendly, low-cost, stable, and highly active catalysts for the non-precious hydrogen evolution reaction (HER) is one of the critical factors for the hydrogen energy economy [51]. Double-transition-metal MXenes (DTM MXenes) have been widely pursued in the advancement of renewable energy storage technology in recent years [52]. It seems that the T_x terminal groups play an effective role in expanding the hydrogen production reaction, which is attributed to the interaction of MXene with the reactants and the creation of more active sites [10]. However, there is still insufficient information on the electrochemical characteristics and thermal stability of bimetallic MXenes. Since pure $M'_2M''C_2$ carbonitrides are surrounded by metal atoms and free electrons, the end terminals easily become electronegative during synthesis, which plays a significant role in charge transfer for hydrogen evolution reaction [10].

Based on the density functional theory (DFT) calculations of Li et al., the performance of mono-metal MXenes is improved by forming a sandwich configuration of double-metal MXene [52]. The results of their research showed that in terms of hydrogen production, carbonitrides made of molybdenum ($Mo_2M''C_2O_2$) are more efficient than chromium-based MXene (M″: Ti, V, Nb, and Ta). As a result of improving the geometric structure, the activity of MXenes promotes the direction of the hydrogen evolution reaction. The ΔG energy of H* adsorption and hydrogen coverage exhibits an intimate relationship to the H_2 production of carbonitrides. Through DFT calculations, Zeng and colleagues have found 11 candidates superior to platinum among 64 ordered DTM oxygen-functionalized MXenes for hydrogen production [53]. Furthermore, Mo_2TiCNO_2, Ti_2VCNO_2, and Ti_2NbCNO_2 have been screened in terms of stability compared to other compounds of this group of MXenes. Among these three compounds, Ti_2NbCNO_2 is more capable of catalytic conversion because it has abundant catalytic sites in carbon and its ΔG is lower in hydrogen absorption. In another research, it has been found the ΔG of H_2 absorption of $Mo_2TiC_2P_2$ and $CrM'C_2S_2$ (M′: Ti and V) with spontaneous conductivity are close to zero, which is a requirement for high catalytic activity in hydrogen production [32]. The difference between the energy level in the vacuum and the Fermi level is known as the work function [54]. In other words, the work function provides

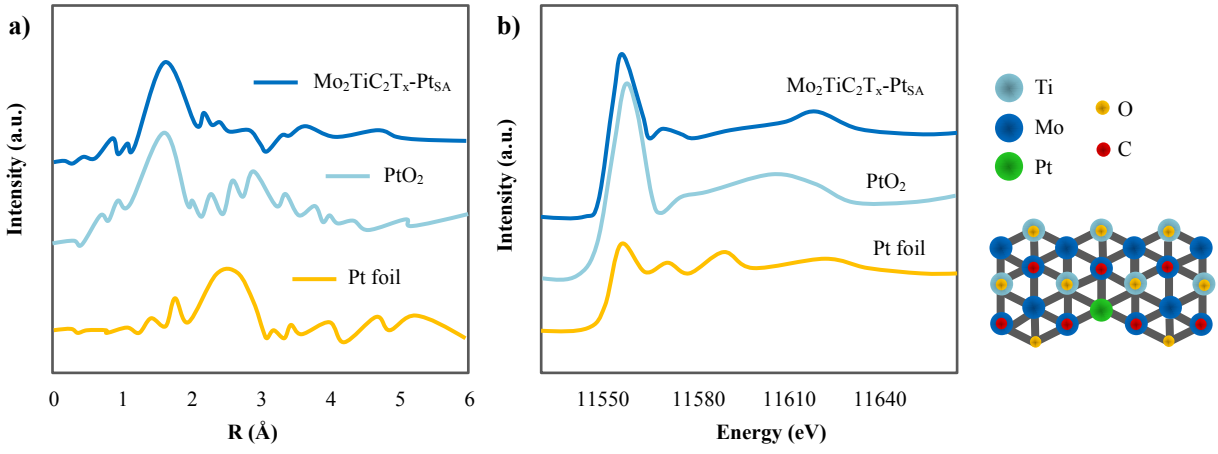

Fig. 7. a) Normalized XANES spectra of $Mo_2TiC_2T_x$–Pt_{SA} and b) the Fourier transform of EXAFS spectra.

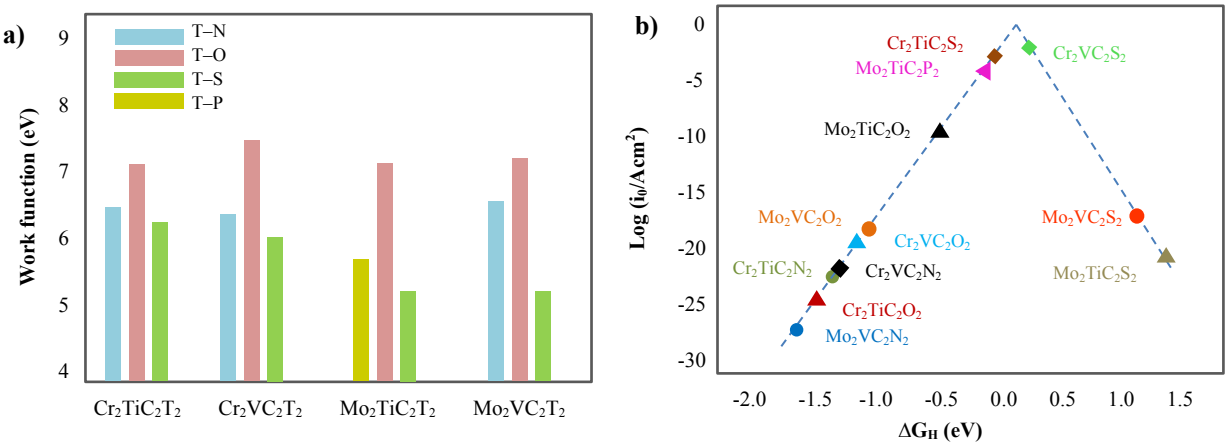

Fig. 8. a) Work function of $M_2M'C_2T_2$ monolayers and b) Volcano curve of exchange current vs. ΔG_H.

an energy barrier against the free space preventing electrons in the Fermi level. As seen in the Fig. 8, terminal atoms can affect the performance of carbonitrides. Functional group –O shows the highest work function in $M_2M'C_2$ monolayers, which strongly connect with internal electrons.

By examining the surface functional group, Sun and colleagues [55] discovered that DTM MXenes can be made semiconducting. In this regard, $TiMn_2N_2$–F has a wide range of properties, which has encouraged practical studies in wide applications. It has been found that $TiMn_2N_2F_2$ is half-metallic with a large bandgap of ~1.1 eV. In another work, O-functionalized DTM carbides have been investigated to estimate elastic, and electronic properties by DFT calculations [56]. It has been found that the elastic features of Mo-based C_2O_2 are superior compared to Cr-based counterparts. In addition, the O-terminated carbides have shown enhanced shear moduli, Young's moduli, and elastic constants compared to the unfunctionalized family. According to a recent theoretical study by Jin et al. [57], it has been determined that the introduction of oxygen vacancies can increase the stability of DTM MXenes modified by a mono metal component such as Au, Ag, Pt, Zn, Cu, Ni, and Co. The stability of surface atoms added to MXenes increases with the introduction of oxygen vacancies, and also ΔG of hydrogen adsorption with metal atoms is adjusted. The reaction mechanism of H_2 desorption changes with the presence of metal atoms and removes the obstacles to the activation of hydrogen production, which leads to the improvement of the catalytic activity. In other research, Zhang et al. [48] have utilized single Pt atoms on $Mo_2TiC_2T_x$ with abundant Mo vacancies to promote the efficiency of catalytic hydrogen evolution. Single atoms trap with the molybdenum vacancy on MXene nanosheets (NSs) and the kinetics of H_2 production is similar to hydrogen evolution by commercial Pt-carbon catalyst. Fig. 9 shows the polarization curve of $Mo_2TiC_2T_x$ with platinum (counter electrode) in order to produce hydrogen in several cycles. Among all samples tested, the $Mo_2TiC_2T_x$/Single Pt atom shows the highest performance, competing with the Pt-carbon catalyst. In

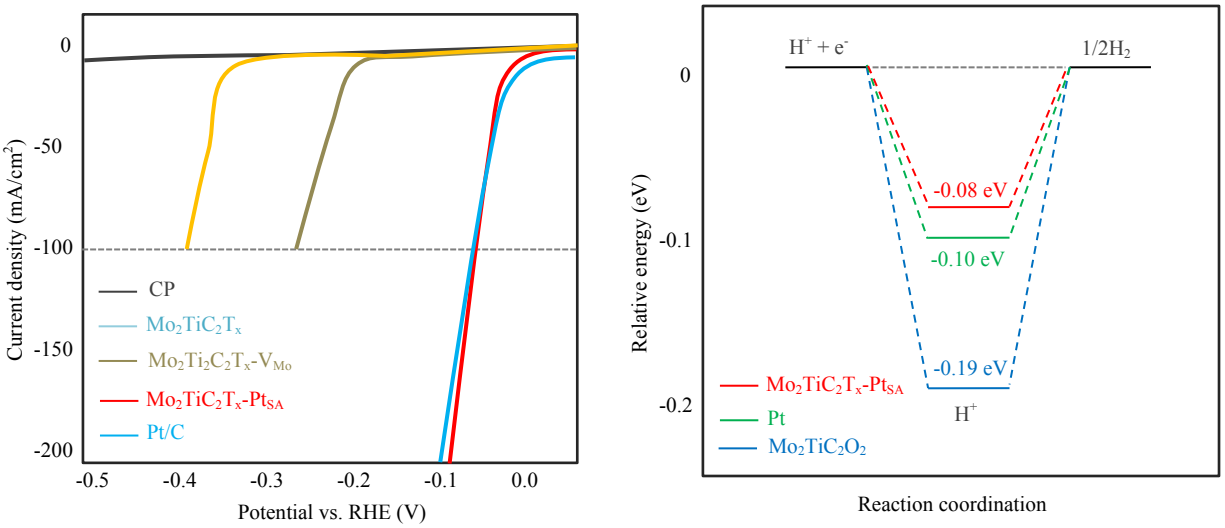

Fig. 9. a) HER polarization curves of $Mo_2TiC_2T_x$ with platinum and b) calculated the free energy profile of HER at the equilibrium potential.

addition, due to the strong covalent interaction between charged platinum atoms and the DTM MXene, this compound exhibits high stability and prevents material aggregation during H_2 evolution. Moreover, Pd/$Mo_2TiC_2T_x$ hybridized with MoS_2 is sufficiently active for electrocatalytic hydrogen evolution in acidic and alkaline electrolytes [58].

Although MXenes are superior to noble metals in water electrolysis for green H_2 production, coordinating both hydrogen and oxygen evolution reactions (OER) is still a challenge. Therefore, Zahra et al. [37] have investigated the dual performance of two types of DTM MXene as an electrocatalyst in alkaline media for overall water splitting. In this regard, they focused on the synthesis of $Mo_2TiC_2T_x$ and $Mo_2Ti_2C_3T_x$ via the wet chemical method. $Mo_2TiC_2T_x$ has shown better oxygen evolution activity with lower overpotential than $Mo_2Ti_2C_3T_x$. Another molybdenum-based DTM MXene is $Mo_{2+\theta}Nb_{2-\theta}C_3T_x$ ($0<\theta<0.3$) with tunable performance for H_2 evolution reaction [34]. It is predicted that Mo-Nb carbonitrides are stable when niobium ions occupy the inner sites according to the Mo-C-Nb-C-Nb-C-Mo arrangements. Among the $Mo_{2+\theta}Nb_{2-\theta}C_3T_x$ derivatives for catalytic hydrogen production, $Mo_{2.28}Nb_{1.6}7C_3T_x$ has the lowest excess potential. In another work, ZIF-67 derived C-N co-doped spongy Co_2P heterostructure has been anchored on $Ti_2VC_2T_x$ for electrocatalytic oxygen evolution reactions [59]. The coupling of DTM MXenes can improve the conductivity and reduce charge transfer resistance. The doped composite has revealed excellent efficiency with low overpotential (410 mV @ 200 mA/cm^2). This strategy and heterostructure engineering could develop on electrocatalytic water splitting.

According to Jin and colleagues' study [60] on 24 double-transition metal carbides including $M_2M'C_2T_x$ and $M_2M_2'C_3T_x$, it is predicted that 18 MXenes are active electrocatalysts to HER. In particular, $Nb_2Ta_2C_3$, $Ti_2M_x'C_y$, and $Mo_2M_x'C_y$ with O-termination are the most stable carbides under standard conditions, while O- and OH-terminated $V_2M_2"C_3$ and $Cr_2M_x"C_y$ are the most stable carbides. As a guide remark, the more fragile the M–O bonds of carbides, the stronger the bond between the adsorbed hydrogen and the terminal -O group. Furthermore, Geng et al. [32] have found that ΔG_H values of $M_2M"C_2T_x$ (T: O and N) monolayers are very negative and also hold very low exchange current. The weak interaction in S–Cr_2TiC_2, S–Cr_2VC_2, and P–Mo_2TiC_2 boosts the H_2 release and causes to very increased exchange current which is useful for H_2 evolution reaction.

4.2. Batteries

For the first time, Mashtalir et al. [61] used MXenes as anodes in lithium batteries and found their excellent charging capacity. The electrochemical intercalations of lithium between carbonitride nanosheets conduct 2D MXenes as favorable solids to construct anodes in Li-ion batteries and capacitors. Not long after, the performance of $Ti_3C_2T_x$ MXene in energy storage was successfully extended by lithium/sodium [62]. However, the limited practical capacity and the tendency of MXenes to accumulate during the electrochemical cycle reduce the efficiency of lithium batteries [63]. DTM carbonitrides are admiringly suitable as an anode in batteries because of their excellent capacity in comparison with conventional single-metal carbonitrides.

Based on the stability of DTM MXenes, MoWC, and $MoWCO_2$ have been chosen by Zhou et al. as the anode in the Na battery in order to store energy [64]. Because the distinct radii of the metal atoms lead to the crystalline lattice of ordered DTM carbonitrides [8], MXenes with excellent properties are formed based on surface engineering, which is suitable for electrode preparation. The molybdenum and tungsten have different radii that could synthesize ordered W–C–Mo MXenes in a large area. The synergy of Mo and W leads to the high capacity of this type of MXenes, and the oxygen functional group does not change it. According to a previous study on W_2C MXene [65], more electrons gathered on the surface of MoWC which leads to a high charge state. It should be mentioned that there are very small diffusion barriers in sodium batteries like lithium batteries [66], which is incompatible with diffusion barriers in Mo_2C [67] and W_2C [65] monolayers. In addition, MoWC monolayers have a high specific capacity of about 670 mAh/g as anode materials for lithium batteries [66]. Moreover, WCrC and $WCrCO_2$ with superior dynamical stability are known as ideal anode materials with ignoble diffusion barriers for the development of sodium-ion batteries [68].

In theoretical research, Li et al. [69] studied the terminated functional group effect on the TiNbC behavior. They found that the –OH group destabilizes $TiNbC(OH)_2$ although it has metallic conductivity. Furthermore, fluorine groups make $TiNbCT_2$ undesirable as an anode material because of the forming of lithium-ion rings. In particular, TiNbC and $TiNbCO_2$ MXenes show distinctive features such as very low lithium diffusion barriers, theoretical storage capacity, and moderate absorption energy comparable to Ti_2C [70] and Nb_2C [71] monolayers, which manifests bimetallic TiNbC and $TiNbCO_2$ are suitable for Li-ion batteries with capacity of 350 and 290 mAhg^{-1}, respectively. In another research, it has been determined that TiNbC and $TiNbCO_2$ have a higher ability than Nb_2C-based single-transition metal MXenes to absorb sodium atoms in a Na-ion battery, which is attributed to the synergistic effect of titanium and niobium, which causes the interaction between the substrate and sodium [72]. In another work, Liu and coworkers [73] have successfully fabricated $Ti_2NbC_2T_x$ as a double transition metal MXene with enlarged interlayer spacing. This anodic material provides fast charge transfer and ion diffusion with a fine capacity of 196 mAh/g which is quite stable during more than 400 cycles.

Previously, the hybridization of single metal MXenes with metallic oxide has been investigated for energy storage in batteries [74]. Therefore, the bimetallic MXenes composite based on metal oxide has been considered. In the studies of Dai et al., $(Ti_{0.9}Nb_{0.1})_3C_2$ has shown a specific capacity of 280 mAh/g at a current density of 0.1 A/g and retains 91.5% of its capacity after 2000 cycles [75]. Hence, the Nb-TiO_2/$(Ti_{0.9}Nb_{0.1})_3C_2$ nanohybrid architecture through an annealing approach leads to a high-performance and stable anode material due to reversible and fast Li ions diffusion and storage with Nb-TiO_2 support. As mentioned, to overcome the unstable structure and limited capacity of 2D MXene, Niobium-doped TiO_2 can be a good choice for anode materials in batteries [40]. In this regard, Nb-doped TiO_2/TiNbC nanolayers prevent structural collapse and reassembly during charge and discharge and promote space Li ions transportation. However, compared to Nb-TiO_2/$(Ti_{0.9}Nb_{0.1})_3C_2$, it has shown a lower reversible performance (260 mAh/g) after 500 cycles. Although TiO_2 is the most widely used semiconductor for the fabrication of hybrid anodic materials, Xu et al. [76] have chosen $VNbO_5$ metallic oxide over $VNbCT_x$. The specific capacity of $VNbO_5$/$VNbCT_x$ is greatly improved compared to V_2O_5 for energy storage in lithium batteries (400 mAh/g> 294 mAh/g). At the same time, other researchers have made a novel 211-phase $VNbCT_x$ by selectively etching the aluminum layer of VNbAlC, which shows a specific capacity of 520 mAh/g with hopeful

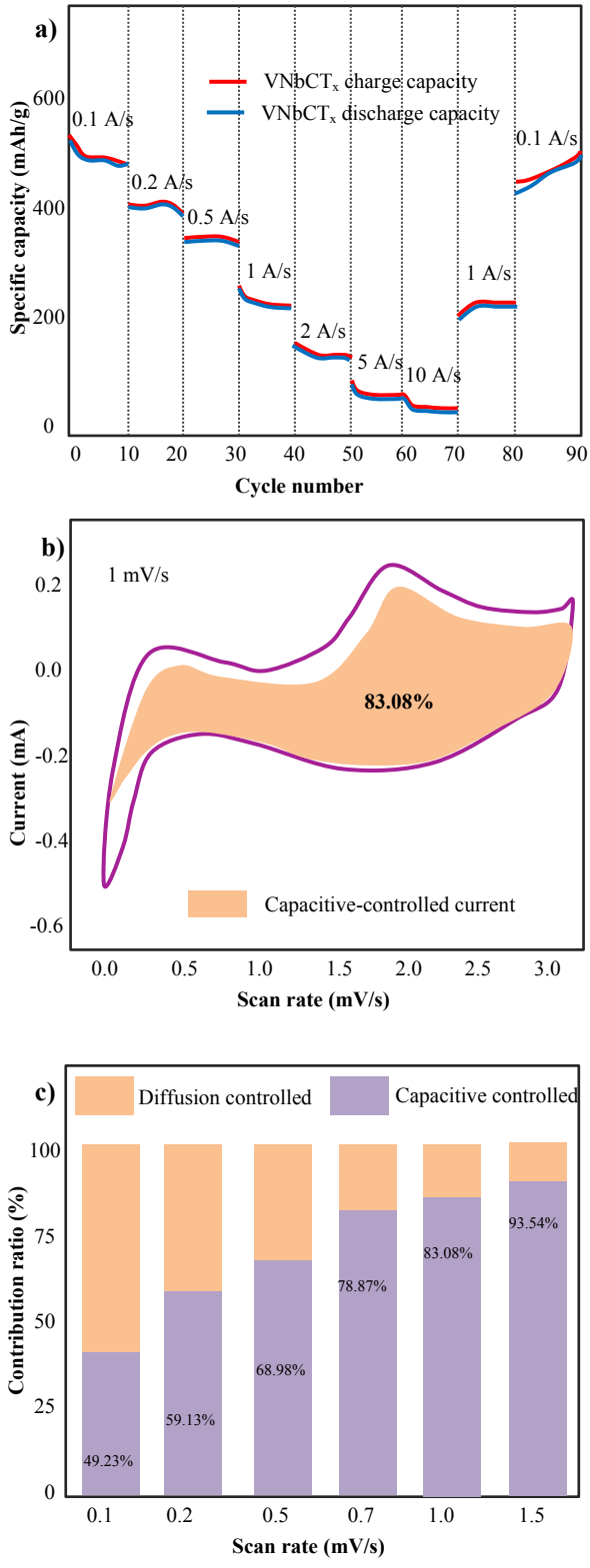

Fig. 10. a) Rate performance of VNbCTx electrode at different current densities, b) CV curves of VNbCTx electrode at a scan rate of 1 mV/s with calculated capacitive-controlled contribution in the shaded region, and c) bar graph depicting capacitive-controlled and diffusion-controlled current contribution at different scan rate.

cycle stability and high rate capability in Li batteries as shown in Fig. 10 [77]. The superior performance is related to the multilayer skeleton of VNbCT$_x$ MXene which can prevent the restacking of mono metal MXene nanosheets. In addition to $VNbO_5$, $TiNbO_x$ is also hybridized as a mixed metal oxide with carbides to obtain a combination with versatile structural and electrochemical properties. For example, Husmann and coworkers [42] have designed and prepared a TiNb-based carbide/$TiNbO_x$ hybrid via thermal oxidation in CO_2 to test as a Li-ion battery electrode. The $TiNbO_x$/TiNbC presented a high 226 mAh/g capacity at 10 mA/g and 75% retention after 1000 cycles at 1 A/g with Nb/Ti: 5 in derived $TiNbO_x$.

Previously, ordered and functionalized TiVC has been investigated through density functional theory calculations and is a candidate anode material for Li-ion batteries [78]. Although all the samples have high electronic conductivity and show metallic characteristics, $TiVCT_2$ functionalized with the sulfur group has shown the lowest barrier to the diffusion of a Li-ion. In addition, in the charge/discharge process, the formation of alkali metal dendrites is prevented by the range of open circuit voltage of lithium ions (0.0–1.0 V) with monolayers of pristine TiVC and $TiVCS_2$. In another work, both ordered and solid-solution structures of TiVC and $TiVCT_2$ have been analyzed as lithium-ion anode materials [79]. In comparison, ordered and solid types of TiVC exhibited excellent adsorptive properties, and the lowest diffusion barriers belong to two different sides of ordered TiVC with the highest theoretical capacity ~480 mAh/g. It is noteworthy that the decreasing trend of TiVC capacity has been observed when it is functionalized with –O, –F, and –OH, respectively. Furthermore, functionalized $TiVCT_x$ blended V_2O_5 and TiO_2 as anode material boosts the Li-ion batteries' performance to 331 mAh/g [80]. In another study, a 3D $TiVCT_x$/poly-o-phenylenediamine composite has been proposed as a chemical and electrochemical stable electrode material in Li-ion batteries [81]. This tremella-like architecture composite has exhibited outstanding properties with a capacity of up to 224 mAh/g at 2 A/g. Compared to the $V_4C_3T_x$/poly-o-phenylenediamine with a capacity of 561 mAh/g at 0.1 A/g [82], the blend of MXenes and conductive polymers is recommended as electrode material. In addition, the TiO_2-based heterostructure of $TiVCT_x$ is a promising strategy for high-performance anode materials [83]. Ti atoms of $Ti_{2-y}V_yCT_x$ could be selectively oxidized on titania particles while V atoms maintain the two-dimensional lamella structure with elevated electronic conductivity. The calculated capacitance contribution is 64% when the scan speed reaches 1 mV/s (Fig. 11). This indicates that the quasi-capacitor control contribution to the total capacity is dominant, which is associated with fast Li^+ storage and superior rate performance.

According to the theory of Tan and coworkers [84], the molybdenum atom prefers to occupy the surface layer in $(M_{1-x}Mo_x)_3C_2$ (where M is Nb, V, Ti, or Ta) and based on Monte Carlo simulation, the ordering continues up to the above temperature. In this regard, Huang and collogues [85] have shown that TiMoC monolayers have low Li-ion diffusion barriers on the titanium surface. Moreover, if chromium is substituted for molybdenum and the concentration of lithium is increased to 2, the theoretical capacity will be 480 mAh/g. In addition, $TiCrCO_2$ displayed a somewhat elevated theoretical capacity of ~370 mAh/g. Therefore, TiCrC, TiMoC, and $TiCrCO_2$ monolayers can be good candidates for the anode material in lithium batteries. Fundamentally, the surface terminations influence the Li-ion adsorption and the theoretical capacity of Mo-based MXenes [86]. Except for –O and –H terminations, it is predicted fast

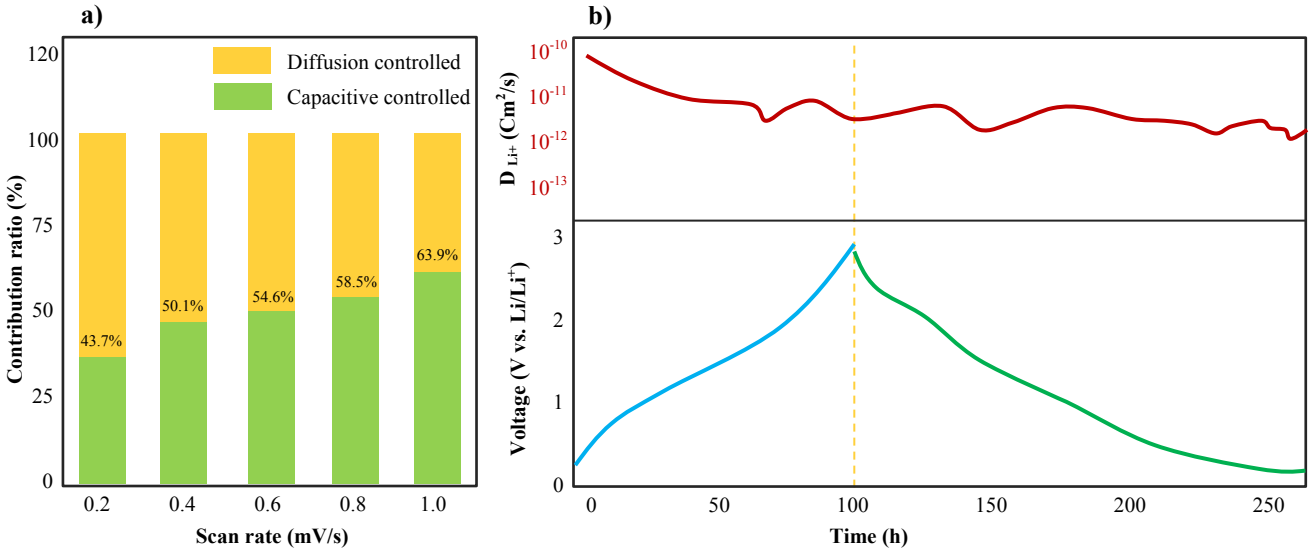

Fig. 11. a) Capacitance contribution of $TiO_2/Ti_{2-y}V_yCT_x$ (1:1) at different scan rates and b) charge/discharge galvanostatic intermittent titration technique curves of $TiO_2/Ti_{2-y}V_yCT_x$ and corresponding lithium ions diffusion coefficient.

charging/discharging process and low barriers of lithium ions (~0.04 eV) for Mo-based MXenes including V, Ti, and Sc.

The main obstacle to large-scale energy storage and conversion systems is the lack of cost-effective, stable, and efficient catalysts. In this regard, NbTaC, VTaC, and VNbC have been designed as double transition metal MXenes with a functionalized terminal to increase anode performance in Na ions batteries [87]. Compared to the single metal counterpart, the Na^+ absorption capacity of NbTaC, VTaC, and VNbC enhances to 75, 37, and 75%, respectively. These composites not only have low initial migration barriers with sodium atoms, but also have high theoretical capacity (NbTaC: 328, VTaC: 302, and VNbC: 602 mAh/g). In another study, $(Nb_yV_{2-y})CT_x$ solid-solution MXene has been explored for energy storage in Li-ion batteries [47]. In lithium-ion batteries, the electrochemical cycling of $Nb_yV_{2-y}C$-derived oxides displayed differing behaviors to V_2C anodes [88].

Of course, single and double layers of nitride-based transition metal containing vanadium and chromium have a bright future in lithium-ion batteries. For example, V_2N and VCrN monolayers have a low energy diffusion barrier of 0.034 and 0.03 eV in Li-ion batteries, respectively [89]. Adsorption of Li-ion multilayers on the upper and lower V_2N/CrVN surfaces results in a specific capacity of 1440.0/1040.0 mAh/g. Further, both mentioned MXenes are thermally stable at 27 and 227 °C. In addition, thallium in DTM Ti-based MXenes has been used as a Li-ion host anode with a remarkable capacity of 460 mAh/g and kept efficiency of around 99% after 200 cycles [90] The great Li-ion storage of the bimetallic $Ti_xTa_{(4-x)}C_3T_x$ could be correlated to the formation of a stable bi-metallic MXene structure, which stores Li-ions on the surface of its layers during the redox reaction. The $Ti_xTa_{(4-x)}C_3T_x$ demonstrated good electronic conductivity between the active materials, carbon additive, and binder, showing good electrochemical properties, remarkable capacity, and great capability [91].

4.3. Magnetic nanodevices

Double transition metal MXenes have semi-metallic properties and intrinsic magnetism that can be used in magnetic and spintronic devices. MXenes research is rapidly evolving to on the application in magnetic devices [92]. Magnetic tunnel junctions called spintronics as nanostructured tools consist of two layers of magnetic metal separated by an ultrathin layer of insulator [93]. These implements are used in the fabrication of magnetic sensors, hard disk drives, magnetic random access memories, etc. [94].

Recently, Cui et al. [95] have employed $ScCr_2C_2F_2$ as the spin-filter tunnel barrier to achieve excellent spin-filtering in the van der Waals magnetic tunnel junction. It has been observed that the $ScCr_2C_2F_2$ monolayers can preserve half-metallicity with good polarization after utilization in magnetic devices. Other Cr-based MXenes, emerging $Mo_2CrN_2O_2$ and $W_2CrN_2O_2$ with varying metallic behaviors and robust ferromagnetism have great potential in electronic devices and nano-spintronics [28]. The direct bandgap of $Mo_2CrN_2O_2$ and $W_2CrN_2O_2$ are 0.77 and 1.35 eV opening up an optimistic future in the preparation of new 2D materials with adjustable magnetic features. It is notable that the bandgap of semiconductors can be predicted using density functional theory (typical errors are <0.1 eV) [96].

A wide group of ordered DTM MXenes such as Ti-V, Ti-Cr, and Ti-Mn with central Ti layers and various terminal groups have been explored by Sun et al. [55]. It has been found that F-terminated $TiMn_2N_2$ has a unique wide bandgap of up to 1.0 eV while the unfunctionalized $TiMn_2N_2$ remains metallic. Therefore, by using wide combinations of bimetallic MXenes, new magnetic, semi-metallic, or insulating behaviors can be achieved with or without surface terminations. Moreover, the magnetic and electronic properties of functionalized $M_2M'C_2T_x$ MXenes (T: S, P, O, N, and B) have been investigated by DFT for use in nanodevices [32]. Based on the stability, a set of DTM MXenes has been screened including $Cr_2VC_2T_x$, $Cr_2TiC_2T_x$, and $Mo_2VC_2T_x$ (T: S, O, and N), which are spontaneously conductive. The magnetic moments of $Cr_2M'C_2T_x$ (M: V and Ti, T: S, O, and N) are mainly contributed by Cr atoms. Differently, S–$Cr_2M'C_2$ (M': Ti and V) monolayers are antiferromagnetic, while $Mo_2VC_2T_x$ (T: S, O, and N) maintain ferromagnetism at ground state with magnetic moment localized on vanadium. These functionalized DTM carbonitrides are favorable composites for magnetic nanodevices.

In another work, $Ti_2MnC_2T_2$ monolayers have been introduced as strong ferromagnetism regardless of surface terminations (T: F, OH, and O) for nanoscale spintronic applications [97]. Both O-terminated Hf_2VC_2 and Hf_2MnC_2 MXenes as 2D robust ferromagnetic materials have high magnetic moments as well as great Curie temperatures based on electron filling in transition-metal cations. Furthermore, Hantanasirisakul et al. [98] have reported comprehensive studies on magnetic as well as electronic properties of $TiCr_2C_2T_x$ MXene for potential spintronic applications. It has been found that a magnetic transition is present in $TiCr_2C_2T_x$ @ around 30 K, which does not exist in its bulk-nanolayered counterpart ($TiCr_2AlC_2$). Besides the Cr cation, the magnetic behavior of the Nb-based 2D MXenes can be observed [99]. For instance, the magnetization of solid solution $(Nb_{1-x}Ti_x)_4C_3$ MXene emerges driven by Ti atoms on the surfaces. In addition, the magnetic features of the mentioned MXene are preserved upon the surface functionalization by OH or F groups. In addition to carbide MXenes, the nitride family has also been proposed for use in electronic devices. WSi_2N_4 and $MoSi_2N_4$, emerging 2D semiconductors, have practical potential for designing energy-efficient and high-performance composites [100, 101].

4.4. Antibacterial

Most of the applications of composites are focused on energy production [102]. Recently, 2D MXenes have been used in biomedical scopes and antibacterial due to their great bio-compatibility and photo-thermal properties. [103]. To overcome bacterial infections and antibiotic resistance, $TiVCT_X$ monolayers have been synthesized and demonstrated their dual-functional antibacterial ability [104]. The Ti-V MXene has exhibited a usual lamellar structure and it also demonstrated above 99.8% antibacterial ability against B. subtilis and E. coli after exposure to low-dose carbide. In addition, the photothermal effect of Ti-V carbide has been examined by NIR laser. Such a double metal MXene showed a stable temperature under 3 times on and off irradiation cycle (Fig. 12), indicating outstanding photothermal stability of $TiVCT_X$.

4.5. Chemical synthesis

One of the crises of the last century is providing affordable energy from renewable sources [105]. Hydrogenation of CO and CO_2 on metal carbide or nitride-based composites is growing as a two-dimensional platform as a substitute for noble metal catalysts to achieve green fuels via various processes [106]. In this regard, Mo, W carbide, and nitride have been used by Patterson et al. [107] as single metal MXene for the Fischer–Tropsch reaction to produce methane as hydrocarbon products in a stirred reactor. Other monometallic MXenes families such as TiC [108] and Nb_2C [109] have been used to reduce CO_2 and methanol production. It has been proven that the lack of functional groups on the surface of molybdenum carbide has a positive effect on the selectivity and activity of MXene [110]. This conclusion cannot be taken in the case of DTM MXenes because the properties and behavior of the bimetallic species are very different. Recently, Wu and his colleagues [111] have effort to reduce the greenhouse gas CO_2 by Ru-Mo_2TiC_2 as a prominent sunlight absorber with a rate of 4 mol/g_{Ru}.h CO production which is 2.5 and 80 times higher than Ru clusters and Ru/SiO_2. Mo-based nitrides have also high potential to be a good composite in the field of photocatalysis [112]. For example, $MoSi_2N_4$ hybridized with $MoSiGeN_4$ has been suggested for photocatalytic CO_2 reduction due to the suitable bandgap of energy.

The commercial conversion of N_2 to urea by CO_2 through the Wöhler synthesis [113] is used to promote energy and environmental strategies. Global urea and ammonia production account above 2% of the world's energy consumption. Therefore, it is necessary to produce urea with high-performance electrocatalysts under moderate conditions. However, the common process suffers from many technical bottlenecks to proceed under mild conditions. In new research, for the first time, Yang and co-workers [114] designed Mo_2VC_2 DTM carbide as a promising electrocatalyst for urea synthesis. Although Mo_2VC_2 has a lower potential than the Cu-Pd catalyst [115], it has opened a bright horizon for nitrogen-to-urea conversion.

Improving the Haber–Bosch process for NH_3 generation via N_2 reduction can reduce greenhouse gas emissions [116]. DFT calculations can screen the effective metal atoms as supporting defective $Mo_2TiC_2O_2$ nanosheets, which significantly promote the N_2 reduction reactions. Recently, doping of $Mo_2TiC_2O_2$ with Zr single atoms has been explored for nitrogen reduction at ambient conditions [117]. The formation energy of Zr-doped $Mo_2TiC_2O_2$ is more negative than synthesized Pt-doped $Mo_2TiC_2O_2$, which indicates the readiness of this composite to be a good candidate for N_2 conversion. It should be noted that in the process of nitrogen reduction, the lowest barrier of the potential determination stage is reported to be 0.15 eV. It has been proved that N_2 molecules could intensely adsorb on DTM carbides and activate for NH_3 production. Another DTM MXene candidate is $Mo_2Nb_2C_3$ with a low overpotential of 0.48 V [118]. Among the 18 MXenes shown in Fig. 13, $Mo_2Nb_2C_3$ has the lowest reaction-free energy of the potential determining step (ΔG_{PDS}). Molybdenum molecules can control the electrons required for the reaction and increase the activity of the N_2 fixation. Combining DFT calculations and Monte Carlo simulation, Fang and his coworkers [119] have introduced 5 potential DTM MXenes consisting of V-Mo, Nb-Cr, Mo-Mn, and Mo-W for N_2 reduction reaction.

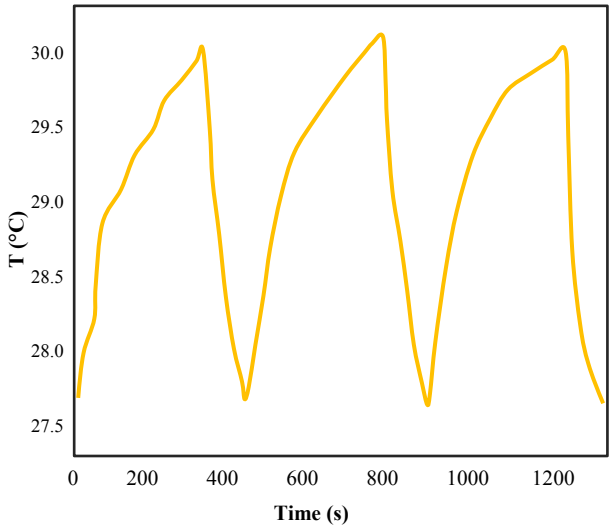

Fig. 12. Photothermal stability of the $TiVCT_X$ under laser irradiation (0.1 W/cm^2, 808 nm, and 40 µg/ ml) for 5 min and operated by turning the laser on and off for 3 cycles.

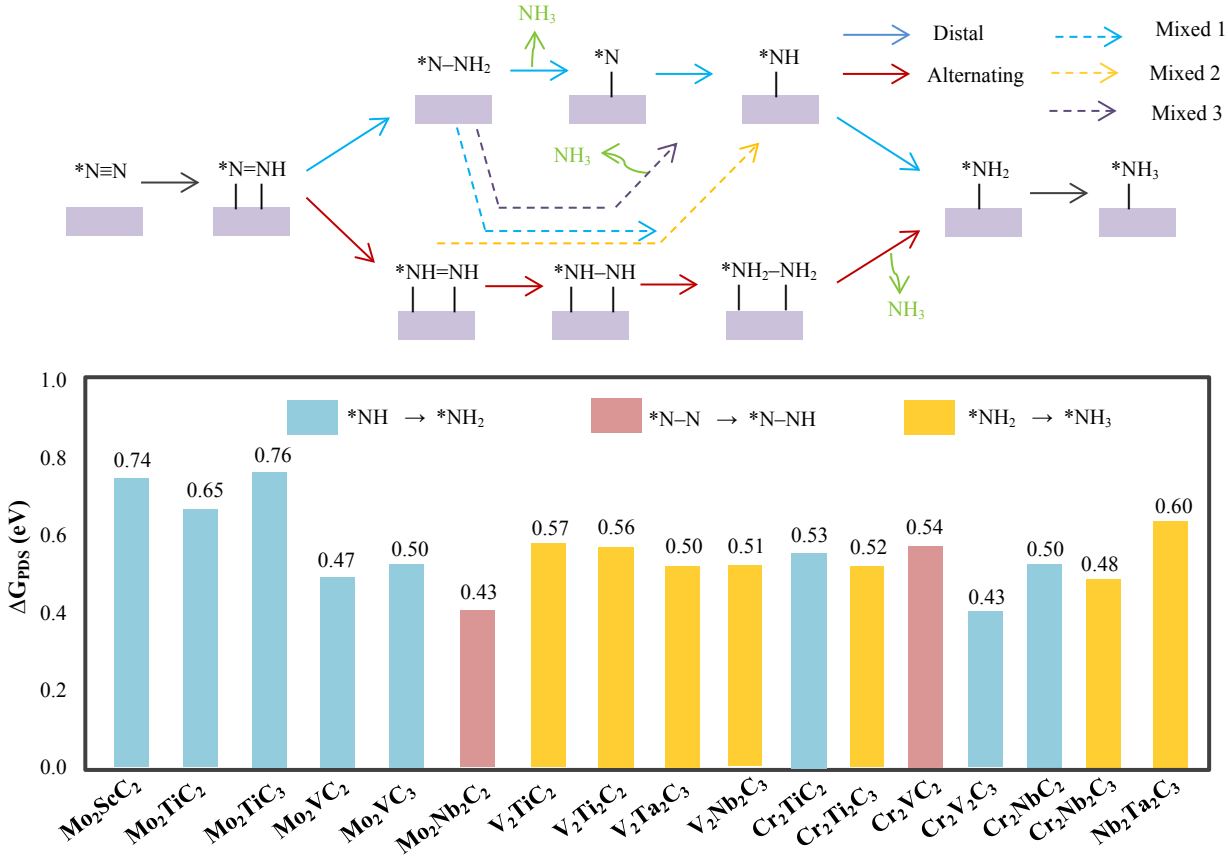

Fig. 13. ΔG_{PDS} for some type of DTM MXenes (color codes represent the corresponding PDS of each step). ΔG_{PDS} for all DTM carbides are below 0.8 eV.

4.6. Sensors and biosensors

The chemical composition and layered structure, and high conductivity of MXenes have made them attractive for the application and development of sensors and biosensors [120]. In addition, 2D MXenes display suitable bandgap, lower current leakage and low diffusion barriers, thereby improving detection sensitivity [121]. Therefore, gas sensors based on MXenes, electrochemical and optical biosensors have been studied and researched. In one case, 2D $MoSi_2N_4$ monolayers have been studied as sensors for, SO_2, NO, NO_2, and O_2 detection [122]. It has been found that the surface of $MoSi_2N_4$ acts as a charge acceptor or donor and all molecules are physically adsorbed on the surface by small charge transfer. With the physisorbtion of gas molecules, the semiconducting property of $MoSi_2N_4$ does not change and the bandgap distance decreases from 1.79 to 1.50 eV. Later, sensing of sulfur-containing gases (SO_2 and H_2S) on $M_2TiC_2T_x$ (M: Cr, Mo; T_x: O, OH, S) layers have been investigated by means of DFT calculation [123]. The physisorbtion of SO2 is stronger on S-terminated Mo_2TiC_2 and Cr_2TiC_2, whereas H_2S has higher adsorption on O-functionalized Mo_2TiC_2 and Cr_2TiC_2 (Fig. 14a). The isobaric surface coverage of SO_2 and H_2S vs. temperature is shown in Fig. 14b. As can be clearly seen in the figure, $Cr_2TiC_2O_2$ and $MoTiC_2O_2$ are able to detect toxic gases containing very dilute sulfur. In another research, Xu et al. [124] investigated the effect of noble metals absorbed on $MoSi_2N_4$ in the field of gas sensor construction and nitrogen oxide removal. They found that Au-based $MoSi_2N_4$ is suitable for sensing O_2, CO, and SO_2 gas molecules, while Pd-based $MoSi_2N_4$ is more capable of detecting NO_2, NO, and N_2 gases, and Ag-based $MoSi_2N_4$ is only useful for SO_2 sensing. Furthermore, the introduction of Pd atoms on $MoSi_2N_4$ increases the photocatalytic ability of NO removal and prevents the disposal of the toxic NO_2 product because the noble metal atoms reduce the bandgap and improve the ability to absorb light. For the first time, Linghu et al. [125] have proposed Cu-$MoSi_2N_4$ monolayers for the adsorption of NH_3 molecules. The process performance has been analyzed via both non-equilibrium Green's function and DFT. The results of electronic transport calculations have shown that although this composite is sensitive to NH_3, CO, NO, and NO_2 gases, it only moderately adsorbs NH_3 at RT.

In a recent study, SnS_2 and Mo_2TiC_2 quantum dots (QDs) have been designed for a novel electrochemiluminescence biosensor to detect gastric cancer [126]. MoTi-MXene quantum dots have a substantial contribution to the luminescence procedure due to their stability and light processing [127]. SnS_2 nanolayers also increase the brightness intensity of MXenes quantum dots due to their large surface area and low dielectric constant [128, 129]. Therefore, SnS_2/Mo_2TiC_2 QDs is a good candidate for biosensor application.

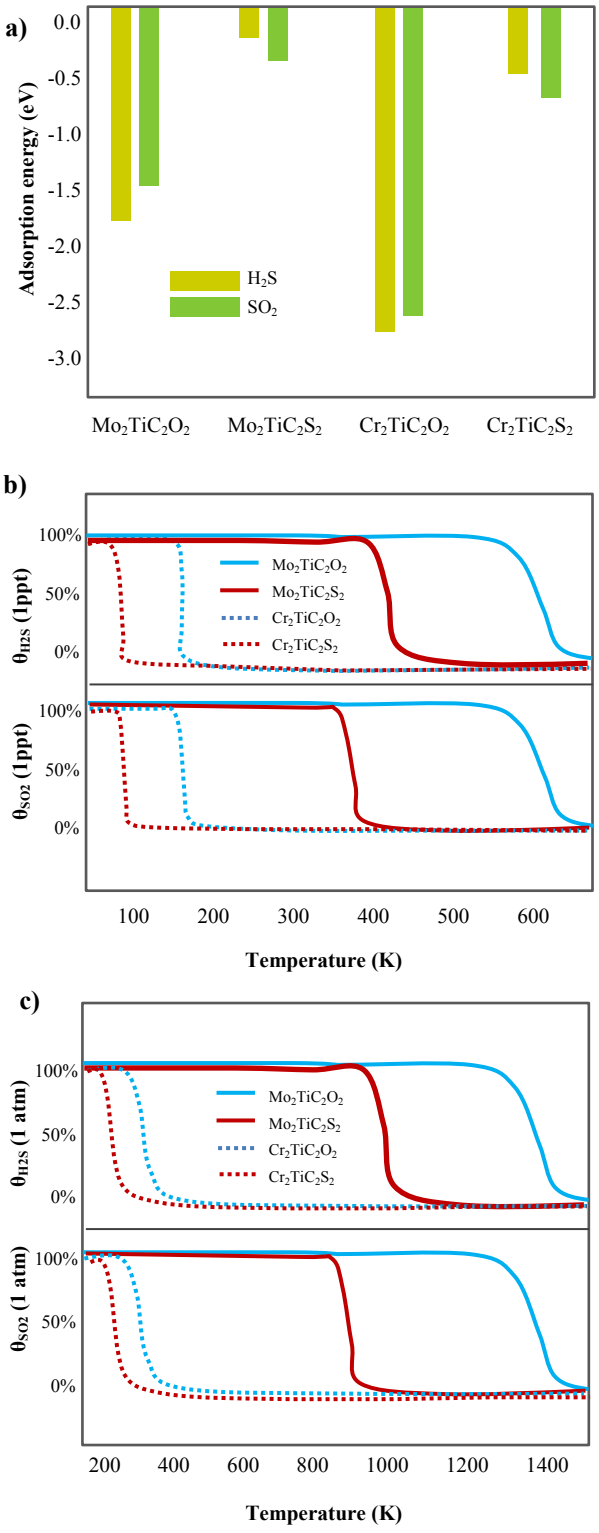

Fig. 14. a) The adsorption energy of H_2S and SO_2 molecules with $Mo_2TiC_2S_2$, $Mo_2TiC_2O_2$, $Cr_2TiC_2S_2$, and $Cr_2TiC_2O_2$ layers and b, c) isobaric surface coverages of SO_2 and H_2S with mentioned MXenes at various temperatures.

5. Conclusions

The selection of metals with a useful hybrid effect has opened new ways for potential applications with desirable properties in the MXenes family. However, the low investigation of physical, mechanical, and electronic characteristics has limited their practical application. The behavior of DTM MXenes is different from single metal MXenes, which can have various uses in the future. This group of two-dimensional materials has greatly helped in designing nanomaterials and meeting new needs. Knowing the electrochemical, metallic, and semiconducting properties of DTM MXenes can ultimately lead to understanding their performance in various applications. Thermodynamic stability is the very first property of the DTM MXenes which is discussed with the role of terminal groups. Most of the MXenes studied have shown metallic properties, thus providing superior charge transport. However, the synthesis of DTM MXenes as newly interesting discovered materials still requires more theoretical and experimental knowledge about characteristics and capabilities.
These results indicate the wide application of bimetallic MXenes from the electrocatalytic production of hydrogen to the anode material in batteries and electronic devices, etc. Various methods have been proposed for the synthesis and preparation of MXenes. Furthermore, the development of new applications is provided with the possibility of structural modification.

CRediT authorship contribution statement

Asieh Akhoondi: Writing – original draft, Resources, Supervision.
Mitra Ebrahimi Nejad: Writing – review & editing.
Mohammad Yusuf: Writing – review & editing.
Tejraj M. Aminabhavi: Writing – review & editing.
Khalid Mujasam Batoo: Writing – review & editing.
Sami Rtimi: Writing – review & editing.

Data availability

As this is a review article, no new data were generated. All information is publicly available or cited appropriately within the article.

Declaration of competing interest

This research received no external funding. The authors have no acknowledgments to declare.

Funding and acknowledgment

This research received no external funding.

References

[1] S. Kanungo, G. Ahmad, P. Sahatiya, A. Mukhopadhyay, S. Chattopadhyay, 2D materials-based nanoscale tunneling field effect transistors: current developments and future prospects, npj 2D Mater. Appl. 6 (2022) 83. https://doi.org/10.1038/s41699-022-00352-2.
[2] D. Er, K. Ghatak, Atomistic modeling by density functional theory of two-dimensional materials, Micro and Nano Technologies, Elseviear. (2020) 113–123. https://doi.org/10.1016/B978-0-12-818475-2.00006-4.
[3] V. Shanmugam, R.A. Mensah, K. Babu, S. Gawusu, A. Chanda, et al., A Review of the Synthesis, Properties, and Applications of 2D

Materials, Part. Part. Syst. Charact. 39 (2022) 2200031. https://doi.org/10.1002/ppsc.202200031.
[4] Z. Xiong, L. Zhong, H. Wang, X. Li, Structural Defects, Mechanical Behaviors, and Properties of Two-Dimensional Materials, Materials. 45 (2021) 1192. https://doi.org/10.3390/ma14051192.
[5] M. Naguib, M. Kurtoglu, V. Presser, J. Lu, J. Niu, et al., Two-Dimensional Nanocrystals Produced by Exfoliation of Ti3AlC2, Adv. Matter. 23 (2011) 4248–4253. https://doi.org/10.1002/adma.201102306.
[6] M. Kurtoglu, M. Naguib, Y. Gogotsi, M.W. Barsoum, First principles study of two-dimensional early transition metal carbides, MRS Commun. 2 (2012) 133–137. https://doi.org/10.1557/mrc.2012.25.
[7] M. Naguib, V.N. Mochalin, M.W. Barsoum, Y. Gogotsi, MXenes: a new family of two-dimensional materials, Adv. Mater. 26 (2014) 992–1005. https://doi.org/10.1002/adma.201304138.
[8] B. Anasori, Y. Xie, M. Beidaghi, J. Lu, B.C. Hosler, et al., Two-Dimensional, Ordered, Double Transition Metals Carbides (MXenes), ACS Nano. 9 (2015) 9507–9516. https://doi.org/10.1021/acsnano.5b03591.
[9] M. Tawalbeh, S. Mohammed, A. Al-Othman, M. Yusuf, M. Mofijur, H. Kamyab, MXenes and MXene-based materials for removal of pharmaceutical compounds from wastewater: Critical review, Environ. Res. 228 (2023) 115919. https://doi.org/10.1016/j.envres.2023.115919.
[10] Y. Cheng, J. Dai, Y. Zhang, Y. Song, Two-Dimensional, Ordered, Double Transition Metal Carbides (MXenes): A New Family of Promising Catalysts for the Hydrogen Evolution Reaction, J. Phys. Chem. C. 122 (2018) 28113–28122. https://doi.org/10.1021/acs.jpcc.8b08914.
[11] M. Zhu, C. Lu, L. Liu, Progress and challenges of emerging MXene based materials for thermoelectric applications, iScience. 26 (2023) 106718. https://doi.org/10.1016/j.isci.2023.106718.
[12] C. Zhang, Y. Zhang, X. Gu, C. Ma, Y. Wang, et al., Radiation synthesis of MXene/Ag nanoparticle hybrids for efficient photothermal conversion of polyurethane films, RSC Adv. 13 (2023) 15157–15164. https://doi.org/10.1039/d3ra02799f.
[13] A. Akhoondi, M. Mirzaei, M.Y. Nassar, Z. Sabaghian, F. Hatami, M. Yusuf, New strategies in the preparation of binary g-C3N4/MXene composites for visible-light-driven photocatalytic applications, Synth. Sinter. 2 (2022) 151–169. https://doi.org/10.53063/synsint.2022.24121.
[14] M. Naguib, J. Halim, J. Lu, K.M. Cook, L. Hultman, et al., New two-dimensional niobium and vanadium carbides as promising materials for Li-ion batteries, J. Am. Chem. Soc. 135 (2013) 15966–15969. https://doi.org/10.1021/ja405735d.
[15] M. Feng, W. Wang, Z. Hu, C. Fan, X. Zhao, et al., Engineering chemical-bonded Ti3C2 MXene@carbon composite films with 3D transportation channels for promoting lithium-ion storage in hybrid capacitors, Sci. China Mater. 66 (2023) 944–954. https://doi.org/10.1007/s40843-022-2268-9.
[16] A. Akhoondi, H. Ghaebi, L. Karuppasamy, M.M. Rahman, P. Sathishkumar, Recent advances in hydrogen production using MXenes-based metal sulfide photocatalysts, Synth. Sinter. 2 (2022) 37–54. https://doi.org/10.53063/synsint.2022.21106.
[17] L. Chen, X. Dai, W. Feng, Y. Chen, Biomedical Applications of MXenes: From Nanomedicine to Biomaterials, Acc. Mater. Res. 3 (2022) 785–798. https://doi.org/10.1021/accountsmr.2c00025.
[18] H. Bark, G. Thangavel, R.J. Liu, D.H.C. Chua, P.S. Lee, Effective Surface Modification of 2D MXene toward Thermal Energy Conversion and Management, Small Methods. 7 (2023) 2300077. https://doi.org/10.1002/smtd.202300077.
[19] W. Hong, B.C. Wyatt, S.K. Nemani, B. Anasori, Double transition-metal MXenes: Atomistic design of two-dimensional carbides and nitrides, MRS Bull. 45 (2020) 850–861. https://doi.org/10.1557/mrs.2020.251.
[20] Z.W. Seh, K.D. Fredrickson, B. Anasori, J. Kibsgaard, A.L. Strickler, et al., Two-Dimensional Molybdenum Carbide (MXene) as an Efficient Electrocatalyst for Hydrogen Evolution, ACS Energy Lett. 1 (2016) 589–594. https://doi.org/10.1021/acsenergylett.6b00247.
[21] M.G. Moreno-Armenta, J. Guerrero-Sánchez, S.J. Gutiérrez-Ojeda, H.N. Fernández-Escamilla, D.M. Hoat, R. Ponce-Pérez, Theoretical investigation of the MXene precursors MoxV4-xAlC3 ($0 \leq x \leq 4$), Sci. Rep. 13 (2023) 3271. https://doi.org/10.1038/s41598-023-30443-z.
[22] A.P. Umanskii, V.A. Lavrenko, S.S. Chuprov, V.P. Konoval, High-temperature oxidation of composites based on titanium carbonitride and double titanium-chromium carbide, Refract. Ind. Ceram. 47 (2006) 246–250. https://doi.org/10.1007/s11148-006-0099-5.
[23] S. Venkateshalu, G.M. Tomboc, B. Kim, J. Li, K. Lee, Ordered Double Transition Metal MXenes, ChemNanoMat. 8 (2022) e202200320. https://doi.org/10.1002/cnma.202200320.
[24] E. Omugbe, O.E. Osafile, O.N. Nenuwe, E.A. Enaibe, E.E. Elemike, Thermal and electrical transport conductivities of novel ordered double two-dimensional MXenes via density functional theory, Can. J. Chem. 101 (2023) 316–325. https://doi.org/10.1139/cjc-2022-0070.
[25] W.-L. Chang, Z.-Q. Sun, Z.-M. Zhang, X.-P. Wei, X. Tao, Thermoelectric properties of two-dimensional double transition metal MXenes: ScYCT2 (T=F, OH), J. Phys. Chem. Solids. 176 (2023) 111210. https://doi.org/10.1016/j.jpcs.2022.111210.
[26] N.M. Caffrey, Prediction of Optimal Synthesis Conditions for the Formation of Ordered Double-Transition-Metal MXenes (o-MXenes), J. Phys. Chem. C. 124 (2020) 18797–18804. https://doi.org/10.1021/acs.jpcc.0c05348.
[27] E. Bolen, E. Deligoz, Computational study of mechanical stability and phonon properties of MXenes Mo2ScC2T2 (T = O and F): 2D materials, J. Appl. Phys. 130 (2021) 065102. https://doi.org/10.1063/5.0055701.
[28] K.D. Dihingia, S. Saikia, N. Yedukondalu, S. Saha, S.G. Narahari, 2D-Double transition metal MXenes for spintronics applications: surface functionalization induced ferromagnetic half-metallic complexes, J. Mater. Chem. C. 10 (2022) 17886–17898. https://doi.org/10.1039/D2TC03067E.
[29] E.M.D. Siriwardane, P. Karki, Y.L. Loh, D. Çakır, Engineering magnetic anisotropy and exchange couplings in double transition metal MXenes via surface defects, J. Phys: Condens. Matter. 33 (2021) 035801. https://doi.org/10.1088/1361-648X/abba8e.
[30] Y. Zhang, C. Zhou, B. Sa, N. Miao, J. Zhou, Z. Sun, Computational design of double transition metal MXenes with intrinsic magnetic properties, Nanoscale Horiz. 7 (2022) 276–287. https://doi.org/10.1039/D1NH00621E.
[31] X. Jiang, A.V. Kuklin, A. Baev, Y. Ge, H. Ågren, et al., Two-dimensional MXenes: From morphological to optical, electric, and magnetic properties and applications, Phys. Rep. 848 (2020) 1–58. https://doi.org/10.1016/j.physrep.2019.12.006.
[32] J. Geng, R. Wu, H. Bai, I.-N. Chan, K.W. Ng, et al., Design of functionalized double-metal MXenes (M2M'C2T2: M = Cr, Mo, M' = Ti, V) for magnetic and catalytic applications, Int. J. Hydrog. Energy. 47 (2022) 18725–18737. https://doi.org/10.1016/j.ijhydene.2022.04.058.
[33] D.R. Kumar, R. Karthik, M. Hasan, M.S. Sayed, J.-J. Shim, Mo-MXene-filled gel polymer electrolyte for high-performance quasi-solid-state zinc metal batteries, Chem. Eng. J. 473 (2023) 145207. https://doi.org/10.1016/j.cej.2023.145207.
[34] B.C. Wyatt, A. Thakur, K. Nykiel, Z.D. Hood, S.P. Adhikari, et al., Design of Atomic Ordering in Mo2Nb2C3Tx MXenes for Hydrogen Evolution Electrocatalysis, Nano Lett. 23 (2023) 931–938. https://doi.org/10.1021/acs.nanolett.2c04287.
[35] K.R.G. Lim, M. Shekhirev, B.C. Wyatt, B. Anasori, Y. Gogotsi, Z. W. Seh, Fundamentals of MXene synthesis, Nat. Synth. 1 (2022) 601–614. https://doi.org/10.1038/s44160-022-00104-6.
[36] Y. Gogotsi, B. Anasori, The Rise of MXenes, ACS Nano. 13 (2019) 8491–8494. https://doi.org/10.1021/acsnano.9b06394.

[37] S.A. Zahra, M.W. Hakim, M.A. Mansoor, S. Rizwan, Two-dimensional double transition metal carbides as superior bifunctional electrocatalysts for overall water splitting, Electrochim. Acta. 434 (2022) 141257. https://doi.org/10.1016/j.electacta.2022.141257.
[38] K. Byrappa, T. Adschiri, Hydrothermal technology for nanotechnology, Prog. Cryst. Growth Charact. Mater. 53 (2007) 117–166. https://doi.org/10.1016/j.pcrysgrow.2007.04.001.
[39] A. Akhoondi, M. Aghaziarati, N. Khandan, Production of highly pure iron disulfide nanoparticles using hydrothermal synthesis method, Appl. Nanosci. 3 (2013) 417–422. https://doi.org/10.1007/s13204-012-0153-1.
[40] Q. Ma, Z. Zhang, P. Kou, D. Wang, Z. Wang, et al., In-situ synthesis of niobium-doped TiO2 nanosheet arrays on double transition metal MXene (TiNbCTx) as stable anode material for lithium-ion batteries, J. Colloid Interface Sci. 617 (2022) 147–155. https://doi.org/10.1016/j.jcis.2022.03.007.
[41] K. Byrappa, N. Keerthiraj, S.M. Byrappa, Hydrothermal Growth of Crystals—Design and Processing, Handbook of Crystal Growth (Second Edition), Elsevier. (2015) 535–575. https://doi.org/10.1016/B978-0-444-63303-3.00014-6.
[42] S. Husmann, M. Besch, B. Ying, A. Tabassum, M. Naguib, V. Presser, Nb Carbides (MXene) as Anode Materials for Li-Ion Batteries, ACS Appl. Energy Mater. 5 (2022) 8132–8142. https://doi.org/10.1021/acsaem.2c00676.
[43] A. Akhoondi, Z. Mahmoud, Khandan Nahid, Hydrothermal Production of Highly Pure Nano Pyrite in a Stirred Reactor, Iran. J. Chem. Chem. Eng. 33 (2014) 15–19. https://doi.org/10.30492/IJCCE.2014.7189.
[44] Y.-T. Liu, P. Zhang, N. Sun, B. Anasori, Q. Zhu, et al., Self-Assembly of Transition Metal Oxide Nanostructures on MXene Nanosheets for Fast and Stable Lithium Storage, Adv. Mater. 30 (2018) 1707334. https://doi.org/10.1002/adma.201707334.
[45] C. Zhang, S.J. Kim, M. Ghidiu, M.Q. Zhao, M.W. Barsoum, et al., Layered Orthorhombic Nb2O5@Nb4C3Tx and TiO2@Ti3C2Tx Hierarchical Composites for High Performance Li-ion Batteries, Adv. Funct. Mater. 26 (2016) 4143–4151. https://doi.org/10.1002/adfm.201600682.
[46]M. Fides, P. Hvizdoš, R. Bystrický, A. Kovalčíková, R. Sedlák, et al., Microstructure, fracture, electrical properties and machinability of SiC-TiNbC composites, J. Eur. Ceram. Soc. 37 (2017) 4315–4322. https://doi.org/10.1016/j.jeurceramsoc.2017.05.004.
[47] M.A. Andrade, T. Averianov, C.E. Shuck, K. Shevchuk, Y. Gogotsi, E. Pomerantseva, Synthesis of 2D Solid-Solution (NbyV2–y)CTx MXenes and Their Transformation into Oxides for Energy Storage, ACS Appl. Nano Mater. 6 (2023) 16168–16178. https://doi.org/10.1021/acsanm.3c02004.
[48] J. Zhang, Y. Zhao, X. Guo, C. Chen, C.-L. Dong, et al., Single platinum atoms immobilized on an MXene as an efficient catalyst for the hydrogen evolution reaction, Nat. Catal. 1 (2018) 985–992. https://doi.org/10.1038/s41929-018-0195-1.
[49] A. Akhoondi, A. Sharma, D. Pathak, M. Yusuf, T.B. Demissie, et al., Hydrogen evolution via noble metals based photocatalysts: A review. Synth. Sinter. 1 (2021) 223–241. https://doi.org/10.53063/synsint.2021.1468.
[50] L. Tian, Z. Li, M. Song, J. Li, Recent progress in water-splitting electrocatalysis mediated by 2D noble metal materials, Nanoscale. 13 (2021) 12088–12101. https://doi.org/10.1039/D1NR02232F.
[51] M. Mirzaei, A. Akhoondi, W. Hamd, J.N. Díaz de León, R. Selvaraj, New updates on vanadate compounds synthesis and visible-light-driven photocatalytic applications, Synth. Sinter. 3 (2023) 28–45. https://doi.org/10.53063/synsint.2023.31132.
[52] N. Li, Z. Zeng, Y. Zhang, X. Chen, Z. Kong, et al., Double Transition Metal Carbides MXenes (D-MXenes) as Promising Electrocatalysts for Hydrogen Reduction Reaction: Ab Initio Calculations, ACS Omega. 6 (2021) 23676–23682. https://doi.org/10.1021/acsomega.1c00870.
[53] Z. Zeng, X. Chen, K. Weng, Y. Wu, P. Zhang, et al., Computational screening study of double transition metal carbonitrides M′2M″CNO2-MXene as catalysts for hydrogen evolution reaction, npj Comput. Mater. 7 (2021) 80. https://doi.org/10.1038/s41524-021-00550-4.
[54] A. Kahn, Fermi level, work function and vacuum level, Mater Horiz. 3 (2016) 7–10. https://doi.org/10.1039/C5MH00160A.
[55] W. Sun, Y. Xie, P. Kent, Double transition metal MXenes with wide band gaps and novel magnetic properties, Nanoscale. 10 (2018) 11962–11968. https://doi.org/10.1039/C8NR00513C.
[56] R. Jayan, A. Vashisth, M.M. Islam, First-principles investigation of elastic and electronic properties of double transition metal carbide MXenes, J. Am. Ceram. Soc. 105 (2022) 4400–4413. https://doi.org/10.1111/jace.18394.
[57] D. Jin, P. Hou, Y. Tian, X. Liu, Y. Xie, et al., Single transition metal atom stabilized on double metal carbide MXenes for hydrogen evolution reaction: a density functional theory study, J. Phys. D: Appl. Phys. 55 (2022) 444002. https://doi.org/10.1088/1361-6463/ac8a5a.
[58] L.-H. Zheng, C.-K. Tang, Q.-F. Lü, J. Wu, MoS2/Mo2TiC2Tx supported Pd nanoparticles as an efficient electrocatalyst for hydrogen evolution reaction in both acidic and alkaline media, Int. J. Hydrog. Energy. 47 (2022) 11739–11749. https://doi.org/10.1016/j.ijhydene.2022.01.201.
[59] J. Li, C. Chen, Z. Lv, W. Ma, M. Wang, et al., Constructing heterostructures of ZIF-67 derived C, N doped Co2P and Ti2VC2Tx MXene for enhanced OER, J. Mater. Sci. Technol. 145 (2023) 74–82. https://doi.org/10.1016/j.jmst.2022.10.048.
[60] D. Jin, L.R. Johnson, A.S. Raman, X. Ming, Y. Gao, et al., Computational Screening of 2D Ordered Double Transition-Metal Carbides (MXenes) as Electrocatalysts for Hydrogen Evolution Reaction, J. Phys. Chem. C. 124 (2020) 10584–10592. https://doi.org/10.1021/acs.jpcc.0c01460.
[61] O. Mashtalir, M. Naguib, V.N. Mochalin, Y. Dall'Agnese, M. Heon, et al., Intercalation and delamination of layered carbides and carbonitrides, Nat. Commun. 4 (2013) 1716. https://doi.org/10.1038/ncomms2664.
[62] X. Song, H. Wang, S. Jin, M. Lv, Y. Zhang, et al., Oligolayered Ti3C2Tx MXene towards high performance lithium/sodium storage, Nano Res. 13 (2020) 1659–1667. https://doi.org/10.1007/s12274-020-2789-6.
[63] K. Kannan, K.K. Sadasivuni, A.M. Abdullah, B. Kumar, Current Trends in MXene-Based Nanomaterials for Energy Storage and Conversion System: A Mini Review, Catalysts. 10 (2020) 495. https://doi.org/10.3390/catal10050495.
[64] M. Zhou, Y. Shen, J.J. Liu, L.L. Lv, Y. Zhang, et al., Excellent double metal MXenes MoWC anode: The synergistic effect of molybdenum and tungsten transition metal, Vacuum. 213 (2023) 112152. https://doi.org/10.1016/j.vacuum.2023.112152.
[65] A. Samad, A. Shafique, H.J. Kim, Y.-H. Shin, Superionic and electronic conductivity in monolayer W2C: ab initio predictions, J. Mater. Chem. A. 5 (2017) 11094–11099. https://doi.org/10.1039/C7TA01177F.
[66] V. Mehta, H.S. Saini, S. Srivastava, M.K. Kashyap, K. Tankeshwar, Ultralow diffusion barrier of double transition metal MoWC monolayer as Li-ion battery anode, J. Mater. Sci. 57 (2022) 10702–10713. https://doi.org/10.1007/s10853-022-07237-1.
[67] Q. Sun, Y. Dai, Y. Ma, T. Jing, W. Wei, B. Huang, Ab Initio Prediction and Characterization of Mo2C Monolayer as Anodes for Lithium-Ion and Sodium-Ion Batteries, J. Phys. Chem. Lett. 7 (2016) 937–943. https://doi.org/10.1021/acs.jpclett.6b00171.
[68] M. Zhou, Y. Shen, J.J. Liu, L.L. Lv, X. Gao, et al., Superionic conductivity and large capacitance behaviors of two-metal MXenes WCrC in sodium ion battery, Vacuum. 200 (2022) 111054. https://doi.org/10.1016/j.vacuum.2022.111054.
[69] Y.-M. Li, W.-G. Chen, Y.-L. Guo, Z.-Y. Jiao, Theoretical investigations of TiNbC MXenes as anode materials for Li-ion

batteries, J. Alloys Compd. 778 (2019) 53–60. https://doi.org/10.1016/j.jallcom.2018.11.140.
[70] S. Zhao, W. Kang, J. Xue, Role of Strain and Concentration on the Li Adsorption and Diffusion Properties on Ti2C Layer, J. Phys. Chem. C. 118 (2014) 14983–14990. https://doi.org/10.1021/jp504493a.
[71] J. Hu, B. Xu, C. Ouyang, Y. Zhang, S.A. Yang, Investigations on Nb2C monolayer as promising anode material for Li or non-Li ion batteries from first-principles calculations, RSC Adv. 6 (2016) 27467–27474. https://doi.org/10.1039/C5RA25028E.
[72] X. Li, Y. Pang, M. Wang, X. Zhang, Z. Lu, Z. Yang, The synergistic effect of Ti and Nb in TiNbC leads to enhanced anode performance for Na-ion batteries - first-principles calculations, Phys. Scr. 98 (2023) 025710. https://doi.org/10.1088/1402-4896/acb46a.
[73] W. Liu, J. Cao, F. Song, D.-D. Zhang, M. Okhawilai, et al., A double transition metal Ti2NbC2Tx MXene for enhanced lithium-ion storage, Rare. Met. 42 (2023) 100–110. https://doi.org/10.1007/s12598-022-02120-z.
[74] X. Guo, X. Xie, S.J. Choi, Y. Zhao, H. Líu, et al., Sb2O3/MXene(Ti3C2Tx) hybrid anode materials with enhanced performance for sodium-ion batteries Sb2O3/MXene(Ti3C2Tx) hybrid anode materials with enhanced performance for sodium-ion batteries, J. Mater. Chem. A. 5 (2017) 12445–12452. https://doi.org/10.1039/C7TA02689G.
[75] Z. Dai, J. Cao, F. Song, D. Zhang, J. Qin, X. Zhang, Architecting Nb-TiO2−x/(Ti0.9Nb0.1)3C2Tx MXene Nanohybrid Anode for High-Performance Lithium-Ion Batteries, Adv. Mater. Interfaces. 9 (2022) 2101658. https://doi.org/10.1002/admi.202101658.
[76] C. Xu, K. Feng, X. Yang, Y. Cheng, X. Zhao, et al., In-situ construction of metallic oxide (VNbO5) on VNbCTx MXene for enhanced Li-ion batteries performance, J. Energy Storage. 69 (2023) 107888. https://doi.org/10.1016/j.est.2023.107888.
[77] Y. Cheng, L. Yang, S. Yin, Synthesis and lithium ion storage performance of novel two dimensional vanadium niobium carbide (VNbCTx) MXene, Compos. Commun. 40 (2023) 101588. https://doi.org/10.1016/j.coco.2023.101588.
[78] Y. Li, L. Li, R. Huang, Y. Zhang, Y. Wen, Computational screening of pristine and functionalized ordered TiVC MXenes as highly efficient anode materials for lithium-ion batteries, Nanoscale. 13 (2021) 2995–3001. https://doi.org/10.1039/D0NR08271F.
[79] S.-P. Huang, J. Zhang, Y.-R. Ren, W.-K. Chen, Investigating the potentials of TiVC MXenes as anode materials for Li-ion batteries by DFT calculations, Appl. Surf. Sci. 569 (2021) 151002. https://doi.org/10.1016/j.apsusc.2021.151002.
[80] K. Feng, Y. Li, C. Xu, M. Zhang, X. Yang, et al., In-situ partial oxidation of TiVCTx derived TiO2 and V2O5 nanocrystals functionalized TiVCTx MXene as anode for lithium-ion batteries, Electrochim. Acta. 444 (2023) 142022. https://doi.org/10.1016/j.electacta.2023.142022.
[81] Y. Li, J. Zhang, Y. Cheng, K. Feng, J. Li, et al., Stable TiVCTx/poly-o-phenylenediamine composites with three-dimensional tremella-like architecture for supercapacitor and Li-ion battery applications, Chem. Eng. J. 433 (2022) 134578. https://doi.org/10.1016/j.cej.2022.134578.
[82] Y. Cheng, Y. Li, L. Yang, S. Yin, Poly(o-phenylenediamine)-Decorated V4C3Tx MXene/Poly(o-phenylenediamine) Blends as Electrode Materials to Boost Storage Capacity for Supercapacitors and Lithium-Ion Batteries, ACS Appl. Nano Mater. 6 (2023) 9186–9196. https://doi.org/10.1021/acsanm.3c00624.
[83] K. Chen, Y. Guan, L. Tan, H. Zhu, Q. Zhang, et al., Atomically selective oxidation of (Ti,V) MXene to construct TiO2@TiVCTx heterojunction for high-performance Li-ion batteries, Appl. Surf. Sci. 617 (2023) 156575. https://doi.org/10.1016/j.apsusc.2023.156575.
[84] T.L. Tan, H.M. Jin, M.B. Sullivan, B. Anasori, Y. Gogotsi, High-Throughput Survey of Ordering Configurations in MXene Alloys Across Compositions and Temperatures, ACS Nano. 23 (2017) 4407–4418. https://doi.org/10.1021/acsnano.6b08227.
[85] S.-P. Huang, J.-F. Gu, Y.-R. Ren, K.-N. Ding, Y. Li, et al., Investigation of Ordered TiMC and TiMCT2 (M = Cr and Mo; T = O and S) MXenes as High-Performance Anode Materials for Lithium-Ion Batteries, J. Phys. Chem. C. 126 (2022) 5283–5291. https://doi.org/10.1021/acs.jpcc.1c10638.
[86] H. Wang, Z. Jing, H. Liu, X. Feng, G. Meng, et al., A high-throughput assessment of the adsorption capacity and Li-ion diffusion dynamics in Mo-based ordered double-transition-metal MXenes as anode materials for fast-charging LIBs, Nanoscale. 12 (2020) 24510–24526. https://doi.org/10.1039/D0NR05828A.
[87] M. Zhou, Y. Shen, J.J. Liu, L.L. Lv, Y. Zhang, et al., Collaborative activation mechanism in double transition metal MXenes anode: An effective method to improve the capacitance of sodium ion battery, Vacuum. 213 (2023) 112150. https://doi.org/10.1016/j.vacuum.2023.112150.
[88] J. Hu, B. Xu, C. Ouyang, S.A. Yang, Y. Yao, Investigations on V2C and V2CX2 (X = F, OH) Monolayer as a Promising Anode Material for Li Ion Batteries from First-Principles Calculations, J. Phys. Chem. C. 118 (2014) 24274–24281. https://doi.org/10.1021/jp507336x.
[89] V. Mehta, H.S. Saini, S. Srivastava, M.K. Kashyap, K. Tankeshwar, N-based single and double transition metal V2N/CrVN monolayers as high capacity anode materials for Li-ion batteries, Mater. Chem. Phys. 290 (2022) 126531. https://doi.org/10.1016/j.matchemphys.2022.126531.
[90] R. Syamsai, J.R. Rodriguez, V.G. Pol, Q.V. Le, K.M. Batoo, et al., Double transition metal MXene (TixTa4−xC3) 2D materials as anodes for Li-ion batteries, Sci. Rep. 11 (2021) 688. https://doi.org/10.1038/s41598-020-79991-8.
[91] M. Naguib, J. Come, B. Dyatkin, V. Presser, P.-L. Taberna, et al., MXene: a promising transition metal carbide anode for lithium-ion batteries, Electrochem. Commun. 16 (2021) 61–64. https://doi.org/10.1016/j.elecom.2012.01.002.
[92] Y.-C. Lin, R. Torsi, R. Younas, C.L. Hinkle, A.F. Rigosi, et al., Recent Advances in 2D Material Theory, Synthesis, Properties, and Applications, ACS Nano. 17 (2023) 9694–9747. https://doi.org/10.1021/acsnano.2c12759.
[93] J.P. Singh, R. Bhardwaj, A. Sharma, B. Kaur, S.O. Won, et al., Fabrication of Magnetic Tunnel Junctions, Advanced Applications in Manufacturing Enginering, Woodhead Publishing. (2019) 53–77. https://doi.org/10.1016/B978-0-08-102414-0.00002-1.
[94] S. Peng, Y. Zhang, M.X. Wang, Y.G. Zhang, W. Zhao, Magnetic Tunnel Junctions for Spintronics: Principles and Applications, Wiley Encyclopedia of Electrical and Electronics Engineering, John Wiley & Sons, Ltd. (2014). https://doi.org/10.1002/047134608X.W8231.
[95] Z. Cui, Y. Zhang, R. Xiong, C. Wen, J. Zhou, et al., Giant tunneling magnetoresistance in two-dimensional magnetic tunnel junctions based on double transition metal MXene ScCr2C2F2, Nanoscale Adv. 4 (2022) 5144–5153. https://doi.org/10.1039/D2NA00623E.
[96] J. Neugebauer, T. Hickel, Density functional theory in materials science, WIREs Comput. Mol. Sci. 3 (2013) 438–448. https://doi.org/10.1002/wcms.1125.
[97] L. Dong, H. Kumar, B. Anasori, Y. Gogotsi, V.B. Shenoy, Rational Design of Two-Dimensional Metallic and Semiconducting Spintronic Materials Based on Ordered Double-Transition-Metal MXenes, J. Phys. Chem. Lett. 8 (2017) 422–428. https://doi.org/10.1021/acs.jpclett.6b02751.
[98] K. Hantanasirisakul, B. Anasori, S. Nemsak, J.L. Hart, J. Wu, et al., Evidence of a magnetic transition in atomically thin Cr2TiC2Tx MXene, Nanoscale Horiz. 5 (2020) 1557–1565. https://doi.org/10.1039/D0NH00343C.
[99] I. Borge-Durán, A. Paul, I. Grinberg, From Non-Magnetic to Magnetic: A First-Principles Study of the Emergence of Magnetism in 2D (Nb1−xTix)4C3 MXenes, Chem. Mater. 35 (2023) 7442–7449. https://doi.org/10.1021/acs.chemmater.3c00367.
[100] Q. Wang, L. Cao, S.-J. Liang, W. Wu, G. Wang, et al., Efficient Ohmic contacts and built-in atomic sublayer protection in MoSi2N4

and WSi2N4 monolayers, npj 2D Mater. Appl. 5 (2021) 71. https://doi.org/10.1038/s41699-021-00251-y.
[101] Q. Wu, L. Cao, Y.S. Ang, L.K. Ang, Semiconductor-to-metal transition in bilayer MoSi2N4 and WSi2N4 with strain and electric field Scilightfeatured, Appl. Phys. Lett. 118 (2021) 113102. https://doi.org/10.1063/5.0044431.
[102] A. Kelly, Composites in context, Compos. Sci. Technol. 23 (1985) 171–199. https://doi.org/10.1016/0266-3538(85)90017-X.
[103] H. Huang, R. Jiang, Y. Feng, H. Ouyang, N. Zhou, et al., Recent development and prospects of surface modification and biomedical applications of MXenes, Nanoscale. 12 (2020) 1325–1338. https://doi.org/10.1039/C9NR07616F.
[104] J. Xi, X. Liu, L. Zhang, Z. Zhang, J. Zhuo, et al., Engineering of Schottky heterojunction in Ru@Bi2S3/Nb2C MXene based on work function with enhanced carrier separation for promoted sterilization, Chem. Eng. J. 473 (2023) 145169. https://doi.org/10.1016/j.cej.2023.145169.
[105] H. Frei, Photocatalytic fuel production, Curr. Opin. Electrochem. 2 (2017) 128–135. https://doi.org/10.1016/j.coelec.2017.03.009.
[106] Z. Qin, T. Su, H. Ji, MXene-Based Photocatalysts Fabrication and Applications, CRC Press., Boca Raton. (2022). https://doi.org/10.1201/9781003156963.
[107] P.M. Patterson, T.K. Das, B.H. Davis, Carbon monoxide hydrogenation over molybdenum and tungsten carbides, Appl. Catal. A. 251 (2003) 449–455. https://doi.org/10.1016/S0926-860X(03)00371-5.
[108] A.B. Vidal, L. Feria, J. Evans, Y. Takahashi, P. Liu, et al., CO2 Activation and Methanol Synthesis on Novel Au/TiC and Cu/TiC Catalysts, J. Phys. Chem. Lett. 3 (2013) 2275–2280. https://doi.org/10.1021/jz300989e.
[109] Y. Cheng, X. Xu, Y. Li, Y. Zhang, Y. Song, CO2 reduction mechanism on the Nb2CO2 MXene surface: Effect of nonmetal and metal modification, Comput. Mater. Sci. 202 (2022) 110971. https://doi.org/10.1016/j.commatsci.2021.110971.
[110] H. Zhou, Z. Chen, E. Kountoupi, A. Tsoukalou, P.M. Abdala, et al., Two-dimensional molybdenum carbide 2D-Mo2C as a superior catalyst for CO2 hydrogenation, Nat. Commun. 12 (2021) 5510. https://doi.org/10.1038/s41467-021-25784-0.
[111] Z. Wu, J. Shen, C. Li, C. Zhang, K. Feng, et al., Mo2TiC2 MXene-Supported Ru Clusters for Efficient Photothermal Reverse Water–Gas Shift, ACS Nano. 17 (2023) 1550–1559. https://doi.org/10.1021/acsnano.2c10707.
[112] N. Mwankemwa, H.-E. Wang, T. Zhu, Q. Fan, F. Zhang, et al., First principles calculations investigation of optoelectronic properties and photocatalytic CO2 reduction of (MoSi2N4)5-n/(MoSiGeN4)n in-plane heterostructures, Results Phys. 37 (2022) 105549. https://doi.org/10.1016/j.rinp.2022.105549.
[113] F. Wöhler, Ueber künstliche Bildung des Harnstoffs, Ann. Phys. Chem. 88 (1828) 253–256. https://doi.org/10.1002/andp.18280880206.
[114] Y. Yang, J. Peng, Z. Shi, P. Zhang, A. Arramel, N. Li, Unveiling the key intermediates in electrocatalytic synthesis of urea with CO2 and N2 coupling reactions on double transition-metal MXenes, J. Mater. Chem. A. 11 (2023) 6428–6439. https://doi.org/10.1039/D2TA09477K.
[115] S. Zhang, J. Geng, Z. Zhao, M. Jin, W. Li, et al., High-efficiency electrosynthesis of urea over bacterial cellulose regulated Pd–Cu bimetallic catalyst, EES. Catal. 1 (2023) 45–53. https://doi.org/10.1039/D2EY00038E.
[116] Z. Li, N.H. Attanayake, J.L. Blackburn, E.M. Miller, Carbon dioxide and nitrogen reduction reactions using 2D transition metal dichalcogenide (TMDC) and carbide/nitride (MXene) catalysts, Energy Environ. Sci. 14 (2021) 6242–6286. https://doi.org/10.1039/D1EE03211A.
[117] L. Li, X. Wang, H. Guo, G. Yao, H. Yu, et al., Theoretical Screening of Single Transition Metal Atoms Embedded in MXene Defects as Superior Electrocatalyst of Nitrogen Reduction Reaction, Small Methods. 3 (2019) 1900337. https://doi.org/10.1002/smtd.201900337.
[118] R. Zhao, Y. Chen, H. Xiang, Y. Guan, C. Yang, et al.,Two-Dimensional Ordered Double-Transition Metal Carbides for the Electrochemical Nitrogen Reduction Reaction, ACS Appl. Mater. Interfaces. 15 (2023) 6797–6806. https://doi.org/10.1021/acsami.2c19911.
[119] Q.-J. Fang, W. Zhang, Q.-j. Zhang, J.-h. Wang, S.-t. Zhao, et al., Rational design of bimetallic MXene solid solution with High-Performance electrocatalytic N2 reduction, J. Colloid Interface Sci. 640 (2023) 67–77. https://doi.org/10.1016/j.jcis.2023.02.094.
[120] R. Khan, S. Andreescu, MXenes-Based Bioanalytical Sensors: Design, Characterization, and Applications, Sensors. 20 (2020) 5434. https://doi.org/10.3390/s20185434.
[121] S. Alwarappan, N. Nesakumar, D. Sun, T. Y. Hu, C.-Z. Li, 2D metal carbides and nitrides (MXenes) for sensors and biosensors, Biosens. Bioelectron. 205 (2022) 113943. https://doi.org/10.1016/j.bios.2021.113943.
[122] A. Bafekry, M. Faraji, M.M. Fadlallah, A. Abdolahzadeh Ziabari, A. Bagheri Khatibani, et al., Adsorption of habitat and industry-relevant molecules on the MoSi2N4 monolayer, Appl. Surf. Sci. 564 (2021) 150326. https://doi.org/10.1016/j.apsusc.2021.150326.
[123] H. Vovusha, R.G. Amorim, H. Bae, S. Lee, T. Hussain, H. Lee, Sensing of sulfur containing toxic gases with double transition metal carbide MXenes, Mater. Today Chem. 30 (2023) 101543. https://doi.org/10.1016/j.mtchem.2023.101543.
[124]. J. Xu, Y. Sun, J. Zeng, F. Zhang, W. Zhang, The electronic and optical properties, gas sensor and NO removal application investigations of noble metal-adsorbed MoSi2N4, Results Phys. 49 (2023) 106481. https://doi.org/10.1016/j.rinp.2023.106481.
[125] Y. Linghu, T. Tong, C. Wu, Cu-Doped MoSi2N4 Monolayer as a Potential NH3 Sensor, ChemPhysChem. 24 (2023) e202200712. https://doi.org/10.1002/cphc.202200712.
[126] M. Li, Z. Li, P. Wang, Q. Ma, A novel bimetallic MXene derivative QD-based ECL sensor for miRNA-27a-3p detection, Biosens. Bioelectron. 228 (2023) 115225. https://doi.org/10.1016/j.bios.2023.115225.
[127] G. Li, B. Zhou, P. Wang, M. He, Z. Fang, et al., High-Efficiency Oxygen Reduction to Hydrogen Peroxide Catalyzed by Oxidized Mo2TiC2 MXene, Catalysts. 12 (2022) 850. https://doi.org/10.3390/catal12080850.
[128] Y. Gao, L. Pan, Q. Wu, X. Zhuang, G. Tan, Q. Man, Honeycomb-like SnS2/graphene oxide composites for enhanced microwave absorption, J. Alloys Compd. 915 (2022) 165405. https://doi.org/10.1016/j.jallcom.2022.165405.
[129] Y. Bao, Y. Liu, Z. Zhang, J. Pan, X. Li, et al., Constructing 2D/2D ultrathin Ti3C2/SnS2 Schottky heterojunctions toward efficient tetracycline degradation, Chemosphere. 307 (2022) 136118. https://doi.org/10.1016/j.chemosphere.2022.136118.